

**THE GEOLOGY, PETROLOGY AND GEOCHEMISTRY  
OF THE PROTEROZOIC INLIER,  
SOUTH OF MYPONGA, FLEURIEU PENINSULA,  
SOUTH AUSTRALIA.**

by

*Peter V. Crowhurst B.Sc.*

Thesis submitted as partial fulfilment for  
the Honours Degree of the Bachelor of Science.  
Department of Geology and Geophysics,  
University of Adelaide,  
November, 1988.

National Grid Reference: Yankalilla Sheet S1-53-6527 (100,000)

# TABLE OF CONTENTS

Page No.

## ABSTRACT

|   |    |
|---|----|
| <b>1. INTRODUCTION</b>                    | 1  |
| 1.1 Location and Physiography             | 1  |
| 1.2 Regional Geology                      | 1  |
| 1.3 Previous Geological Investigations    | 3  |
| 1.4 Aims of Study                         | 4  |
| 1.5 Methods of Study                      | 4  |
| <b>2. LITHOLOGIES AND PETROGRAPHY</b>     | 5  |
| 2.1 Stratigraphy                          | 5  |
| 2.2 Lithologies                           | 5  |
| 2.2.1 Gneisses                            | 5  |
| 2.2.2 Schists                             | 6  |
| 2.2.3 Intrusives                          | 7  |
| 2.2.4 Other lithologies                   | 8  |
| 2.3 Petrography                           | 9  |
| 2.3.1 Gneisses                            | 9  |
| 2.3.2 Schists                             | 11 |
| 2.3.3 Intrusives                          | 12 |
| <b>3. GEOCHEMISTRY</b>                    | 13 |
| 3.1 Introduction                          | 13 |
| 3.2 Amphibolite                           | 13 |
| 3.3 Pegmatite and Aplite                  | 14 |
| 3.4 The 'Houghton' Granulite              | 14 |
| 3.5 Discussions                           | 15 |
| <b>4. STRUCTURE AND METAMORPHISM</b>      | 16 |
| 4.1 Structure                             | 16 |
| 4.2 Metamorphism                          | 18 |
| <b>5. GEOTHERMOMETRY AND GEOBAROMETRY</b> | 20 |
| 5.1 Introduction                          | 20 |
| 5.2 Geothermometry                        | 20 |
| 5.3 Geobarometry                          | 23 |
| <b>6. GEOCHRONOLOGY</b>                   | 25 |
| 6.1 Purpose for Dating                    | 25 |
| 6.2 Sampling and Dating Procedure         | 25 |
| 6.3 Results                               | 26 |
| 6.4 Interpretation and Implication        | 27 |
| <b>7. DISCUSSION AND CONCLUSIONS</b>      | 28 |
| 7.1 Comparison to other basement of S.A   | 28 |

## ACKNOWLEDGEMENTS

## REFERENCES

## LISTS OF APPENDICES

Appendix 1 - Sample locality and observation map, modal analysis, hand specimen and thin section description.

Appendix 2 - Geochemical Analysis a) method of whole rock analysis, b) major and trace element analysis and normative compositions.

Appendix 3 - Electron microprobe analysis and mineral compositions.

Appendix 4 - Geothermometry and Geobarometry.

Appendix 5 - Geochronological techniques and detailed results.

## **LIST OF FIGURES, PLATES AND TABLES.**

- Figure 1. Locality map  
Figure 2. Geology of part of the Yankalilla Map Sheet  
Figure 3-12. Discrimination diagrams using major and trace elements  
Figure 13. Harker diagrams  
Figure 14 Feldspar liquidus under different pressure conditions  
Figure 15. Ternary diagrams showing the mineral assemblage in the amphibolite grade metamorphic pelites from the field area  
Figure 16. P-T diagram of the thermodynamic data from chapter five  
Figure 17. Concordia diagram showing data points of six zircon populations from the Leura Hills Aplite.  
Figure 18. Geology of part of Yankalilla-Myponga Inlier, S.A.
- Table 1 Amphibolite compared to other basic rocks  
Table 2 'Houghton' granulite compared to some basic rocks and some sedimentary rocks  
Table 3 Microprobe data  
Table 4 Garnet biotite geothermometry  
Table 5 U-Pb isotopic analyses of zircon fractions from the Leura Hills Aplite  
Table 6 Myponga Yankalilla Inlier compared to other basement areas of South Australia.

## **PHOTOGRAPHIC PLATES**

- Plate 1 Field photographs  
Plate 2 Field photographs  
Plate 3 Photomicrographs  
Plate 4 Field photographs

## ABSTRACT

The study area is located within the Yankalilla-Myponga Proterozoic Inlier, approximately 60km south of Adelaide. The basement rocks are comprised of a mixture of metasediments and intrusives. The metasediments predominantly comprise of quartz-biotite gneisses and schists. They are intruded by basic dykes, pegmatites and an aplite/microgranite.

The basic dykes have oceanic basalt affinities and could originally been formed during an 'aborted rifting' event, but the more felsic rocks are more likely to be within plate granites. The origin of the 'Houghton' granulite is difficult to ascertain, because it has a varied internal composition and is closely comparable to a diorite and a shale.

The basement inlier rocks are found within the overlying unconformable upper Proterozoic Adelaidean System. They have undergone at least four phases of deformation and metamorphism. Mineral assemblages found in the rocks indicate metamorphism reached at least upper amphibolite facies.

The maximum pressure and temperature conditions were calculated from microprobe data. They range from 8-10 kb at 550 -650 C.

U-Pb isochron dating was performed on the aplite /microgranite of the area and was found to be  $1578 \pm 22$  Ma, which places a minimum age on the inlier rocks.

This date obtained and the deformation processes recognized are comparable to other basement rocks in South Australia; noticeably the Gawler Craton and the Olary Province. This may indicate a homogeneous terrain once spanned most of South Australia during the lower Proterozoic.

## **INTRODUCTION**

### **1.1 Location and Physiography of the Study Area**

The study area is located in the Southern Mount Lofty Ranges approximately 60km south of Adelaide (fig. 1.). The area mapped is part of a basement inlier that is located within the overlying unconformable upper Proterozoic Adelaidean System (fig. 2.).

The basement block south of Myponga forms a S-W to N-E trending range of hills of moderate relief, dissected by semi-permanent streams. It is mainly grazing land with areas of dense natural vegetation. The high grade gneisses and schists that make up the inlier form the terrain of higher relief and are mostly covered by thick scrub in this particular map area. The flatter, grazing area consists mainly of Permian and Quaternary alluvial deposits. The map area is approximately eight square kilometres in size.

### **1.2 Regional Geology**

The basement inliers are found in the Adelaide Geosyncline. The Geosyncline consists mainly of rocks from the Proterozoic Adelaidean System. The Adelaide System overlies with sharp unconformity a basement of gneisses and schists invaded by acid and basic igneous rocks and forming elliptical inliers in the more central portions of the ranges. The Mt.Lofty chain is a faulted anticlinorium with crystalline rocks as cores and Proterozoic-Cambrian sediments as limbs of the folds. An axial culmination is this anticlinorium which brings the basement to the surface. (Campana,1955b).

There are five inliers to be found in the Mount Lofty Ranges, which are all very similar to the study area . They may be distinguished from north to south as the Houghton-Barossa Inlier, Crafers-Aldgate Inlier, Mt.Compass Inlier, Yankalilla-Myponga Inlier and Normanville Inlier ( Glaessner & Parkin, 1958 ).

The inliers consist of a complex suite of metamorphic rocks, of which stressed granite gneisses and migmatites are the most common types. The schists are

comprised of quartz-sericite, quartz-chlorite, plagioclase-quartz-sericite and pyritic varieties, with subordinate bands of kyanite and sillimanite schists. Recrystallized, originally argillaceous, sandstone appear to have produced well-banded gneisses, composed of quartz, mica and chlorite, with occasional grains of tourmaline, zircon and apatite. Many of the gneisses also contain sillimanite and garnet (Glaessner & Parkin, 1958).

Evidence of sedimentary structures has been observed suggesting that the schists and gneisses are derived from sediments ( McEwin, 1972 ).

Granitoid rocks are not uncommon and are to be found invading the metasediments. They are often kaolinized and vary from a pegmatitic-albitic leucogranite to a normal potassic granite (Glaessner *et al.*, 1958 ).

Microdiorites occur as sills or dykes in limited quantity. A more common and characteristic rock of the crystalline suite is the so-called 'Houghton' granulite. Most recent description of the rock describes it as being a Quartz-feldspar gneiss ( Davies, 1972). It varies from being an epidote-bearing banded gneiss to a structureless albite, amphibole-pyroxene granulite, with quartz, hornblende, biotite, apatite, zircon, sphene and rutile as accessory constituents ( McEwin, 1972). Davies (1972) suggests that the 'Houghton' granulite is of sedimentary origin. It is conformable to the surrounding gneisses and has no obvious igneous features.

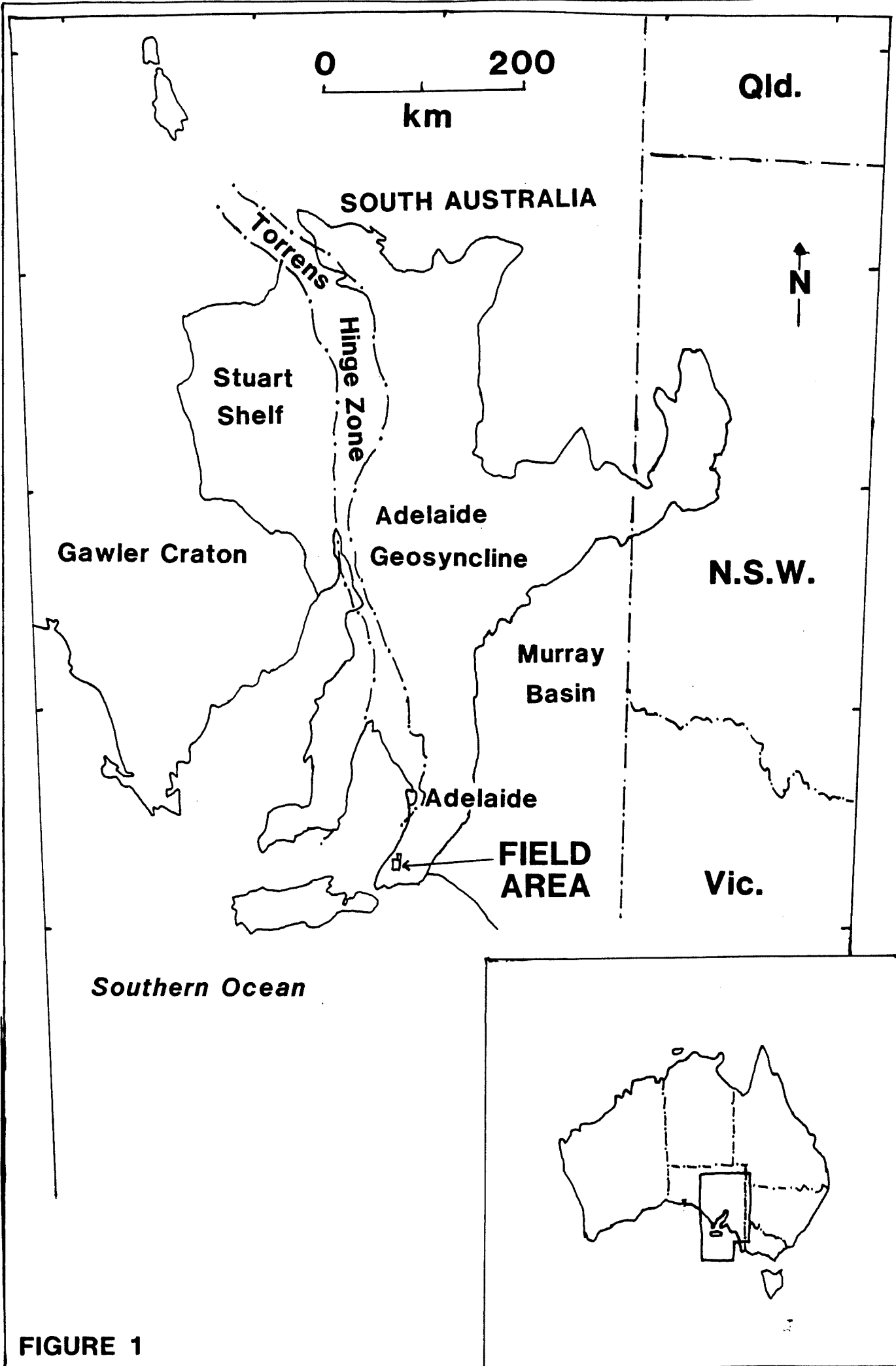
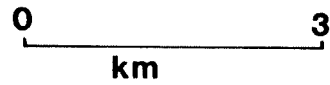


**FIGURE 1**

# LOCALITY MAP

**FIGURE 2 GEOLOGY OF PART OF THE YANKALILLA MAP SHEET**

**REFERENCE**



MAP AREA



**Qrs: Quarternary alluvial flats**

**P: Permian: glacials to sandstones**

**Ck: Cambrian: Kanmantoo Group**

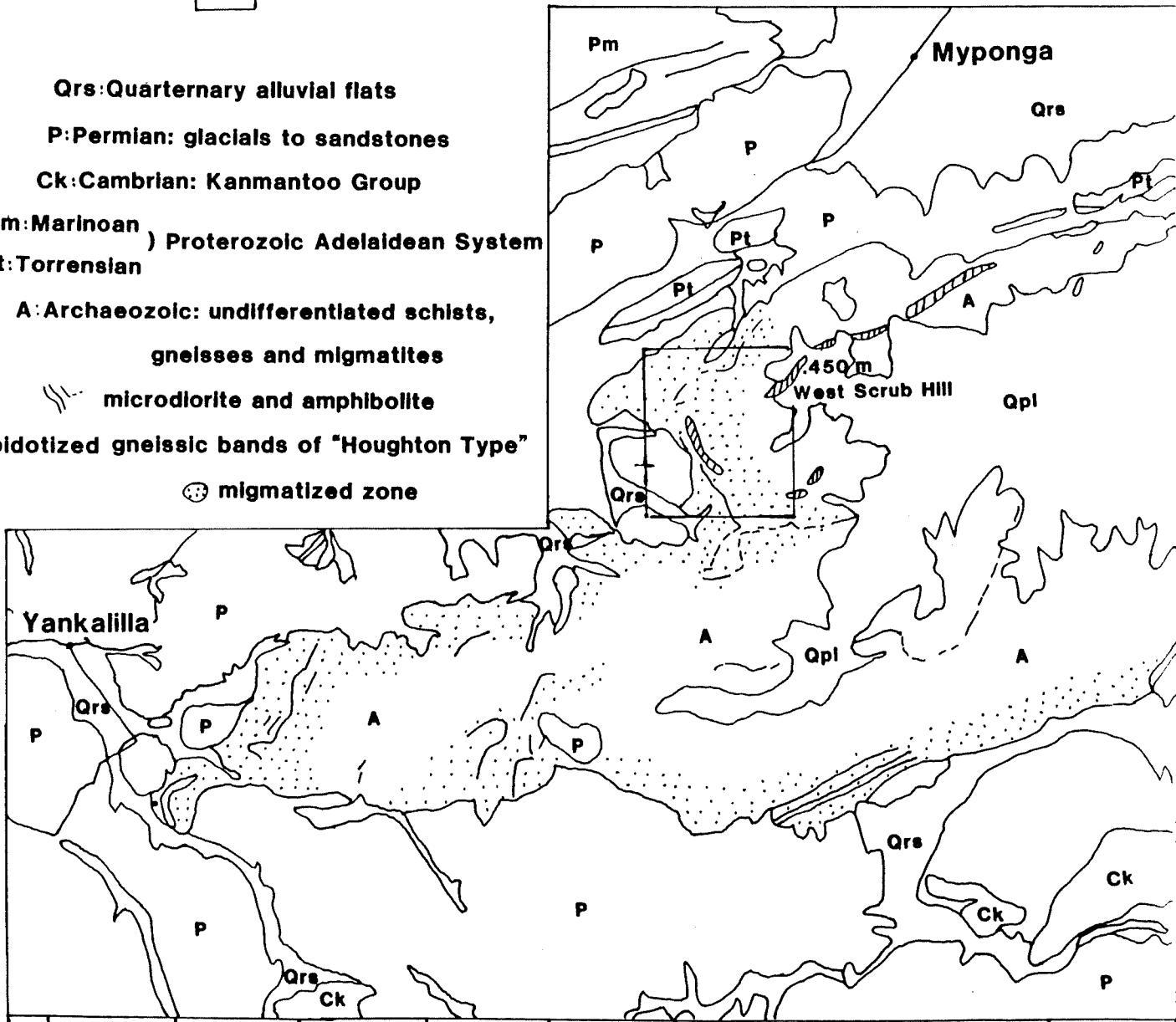
**Pm: Marinoan ) Proterozoic Adelaidean System**  
**Pt: Torrensian**

**A: Archaeozoic: undifferentiated schists, gneisses and migmatites**

microdiorite and amphibolite

Epidotized gneissic bands of "Houghton Type"

migmatized zone





### 1.3 Previous Geological Investigations

The origin and age of the Mount Lofty Inlier rocks has been a subject of debate since 1885 when Brown and Woodward first described a group of gneisses, believed to be possibly Silurian, in the Humbug Scrub. A further brief mention of the same rocks was made by Howchin (1906), who, because of their highly folded and metamorphosed condition, related them to the Archaean.

Benson (1909) first described one of the inliers distinctive rock types, which he called the "Houghton Diorite" and referred to it as being Proterozoic in age. England (1935) demonstrated the chemical similarity of some of the rocks from various parts of the state, then believed to be Archaean in age. Hossfeld (1935) discussed some of the gneisses from Houghton as being sedimentary in nature. Also, Spry (1951) described the "Houghton Diorite" as being a marl-type sediment in origin and not igneous. McEwin (1972), Wicks (1972) and Davies (1972) geochemical analyses also indicate a sedimentary origin for the gneisses, and they also suggest a high grade of metamorphism occurred. Later Forbes (1979) mapped and described the lithologies of the Houghton Inlier.

Early attempts to date the basement rocks to the Adelaide Geosyncline by U-Pb measurements on U minerals (Kleeman, 1946; Campana, 1954; Greenhalgh & Jeffery, 1959) demonstrated the effects of Palaeozoic tectonic events overprinting the basement ages. Only Thomas (1924) was able to obtain an age that would be considered as Proterozoic, (1,073Ma for a pegmatite near Normanville), but the results of his primitive methods were considered doubtful.

Cooper & Compston (1971) carried out whole-rock Rb-Sr dating on the 'Houghton' granulite, calc-silicate rocks from the Houghton Inlier and obtained an age of around 850Ma. This was interpreted as the time of the amphibolite grade metamorphic event described by Talbot (1963). Radke & Webb (1975) derived a date of around 850Ma on the Quartz-feldspar gneiss. Dating attempt by Fanning (1984)

and Fanning *et al.* (1986) gave a poorly defined Delamerian age. Thus this information shows a strong Palaeozoic overprinting effect.

Hence, while early authors estimated the rocks to be Archaean in age and part of the Barossa Complex of rocks, more recent estimates have assigned the rocks to the Proterozoic.

#### **1.4 AIMS OF STUDY**

**1.4.1** To produce a geological map at the scale of 1:4000 of the study area.

**1.4.2** To investigate the petrography and geochemistry of the rocks to determine the metamorphic history and origin.

**1.4.3** To estimate the pressure and temperature conditions the gneissic rocks underwent during metamorphism.

**1.4.4** To obtain a minimum age to the basement rocks of the study area.

#### **1.5 METHODS OF STUDY**

**1.5.1** A colour aerial photograph of 1:16000 scale, together with black and white enlargements of 1:4000 scale were used to map the study area.

**1.5.2** Twenty thin sections were described petrographically.

**1.5.3** Geochemical analysis of 13 samples representative of the lithologies in the study area.

**1.5.4** U-Pb isotopic analysis of zircons extracted from undeformed aplite.

**1.5.5** Microprobe analysis of 6 selected thin sections to obtain information to approximate pressure and temperature conditions of the early high grade metamorphism.

## **2. LITHOLOGIES AND PETROGRAPHY**

### **2.1 Stratigraphy**

The original stratigraphy is generally lost due to the high metamorphism and gross deformation. McEwin (1972) observed repetition of layers in his field area, due to tight isoclinal folding and suggests the 'Houghton' granulite margins can be mapped as it represents part of the original stratigraphy.

### **2.2 Lithologies**

A general classification under four sub-divisions summarizes the rocks in this area;

- (1) two major metasediments - the gneisses and schists, and
- (2) two minor intrusives - pegmatites and amphibolites, plus one minor aplite/microgranite occurrence.

A continuous gradation exists between the schists and gneisses depending on the relative mica, quartz and feldspar content.

#### **2.2.1 Gneisses**

The gneisses form approximately 40-50% of the total area. They vary from a generally light -coloured rock with quartzo-feldspathic bands alternating with darker micaceous bands, to a more massive coarse-grained quartzo-feldspathic rock with little apparent layering. Three distinct types are described below. There is a subtle gradation between these three types rather than any distinct boundaries or stratigraphic succession. The rocks were badly weathered and crumbly as a result of block faulting/jointing that is evident over most of the area.

- (1) The darkest of the three gneiss types, the quartz-biotite gneiss where preferential layering of alternate quartz-feldspar to micaceous layers is exhibited. It is a medium to coarse grained rock. The lighter coloured layers show reasonably equigranular crystals of quartz and feldspar. The more micaceous layers are dominated by biotite which show a preferential orientation of the crystals. The dark

biotite is intergrown with a large percentage of feldspar-like material. Augen structures are common, where quartz and feldspar lenses appear stretched and are surrounded by, or wrapped in by the more micaceous layers.

(2) A sillimanite-bearing gneiss, which is a variation of the above and is a medium-grained rock with occasional coarse-grained augens of quartz and feldspar, and shows a more distinct foliation. This foliation is most likely due to the appearance of fine to medium-grained fibrous material, which in hand specimen resembles sillimanite, but was subsequently identified as a mass of elongate quartz crystals which show a coarse rod-like mineral lineation ( plate 1a ).

(3) The quartzo-feldspathic gneiss is a light coloured, predominantly coarse-grained quartz and feldspar rock. It shows little of the distinct lineation and preferential layering of the other gneissic rocks. It is a massive, reasonably equigranular rock and exhibits signs of retrograde metamorphism, with the feldspar appearing distinctly altered and may have caused the rock to disintegrate under intense weathering.

An epidote-bearing variant of this quartzo-feldspathic gneiss was observed in several localities in the study area. It varies from an epidote-bearing, banded gneiss to a structureless, crystalline, almost granulitic rock containing quartz, feldspar and dark green diopside ( plate 1d ).

### **2.2.2 Schists**

The schists show strong schistosity. They are commonly lineated and both fine to coarse-grained. Segregation banding is prominent in the latter. Micaceous minerals are abundant and show preferred orientation. Some are well-foliated, and coarse grained augens are common. The augens are wrapped by mica and exhibit fracturing. There is a subtle gradation between the schists and gneisses which suggests that some of the schists resulted from shearing and retrogradation of the gneiss. They constitute at least 30-40% of the map area ( plate 1d ).

The migmatites in the area are partially-melted biotite gneisses. These rocks show no continuous layering of the preferential segregation of the minerals, instead the layering is very irregular in length and width. There are sharp boundaries of separation between the felsic and mafic components, contrasting with the gradational variation found in the gneisses. They are variable in grain size, but probably finer grained than the gneisses on average.

### 2.2.3 Intrusives

An Amphibolite/dolerite dyke cuts right across most of the terrain. It is relatively undeformed and appears as a massive, dark, equigranular crystalline rock. It is fine to medium-grained and consists of a white feldspar and a dark, dull mineral which is a pyroxene, altered in part to an amphibole. There seems to be little quartz and the rock shows no layering or lineations of minerals (plate 1c).

The pegmatites in the area vary from relatively large bodies of very coarse-grained, crystalline, massive rock which are predominantly quartz and feldspar rich, to a coarse-grained, crystalline, variably sheared rock which contains significantly more biotite (plate 1b). The sheared pegmatite shows signs of partial melting, with some partial separation of components. They are distinguished from the migmatites by the large grain size and because the boundaries between felsic and mafic components are not sharp (plate 2d).

The plates (2b & 2c) show two phases of pegmatite, the younger intruding the older as well as the basement gneisses. Cross-cutting shear zones are also shown (plate 2a). The pegmatites are quite voluminous and constitute at least 10% of the map area.

The aplite/microgranite rock occurs only as a small intrusion isolated in the gneissic terrain. It is light-coloured consisting predominantly of quartz and pink feldspar with random interspersions of biotite. It is a medium-grained, equigranular, crystalline igneous rock that shows no obvious signs of deformation. It may be related to the later pegmatites.

#### **2.2.4 Other Lithologies**

Other rock types in the area include the Permian and Quaternary deposits that surround the Proterozoic Inlier rocks. To the east of the map area, there is a lateritic crust of the uplifted plateau ( Thomson & Horwitz, 1962), which is Quaternary in age. To the west are undifferentiated Permian deposits, dominantly sandy till and sandstones, which are partly redistributed.

PLATE 1 FIELD PHOTOGRAPHS

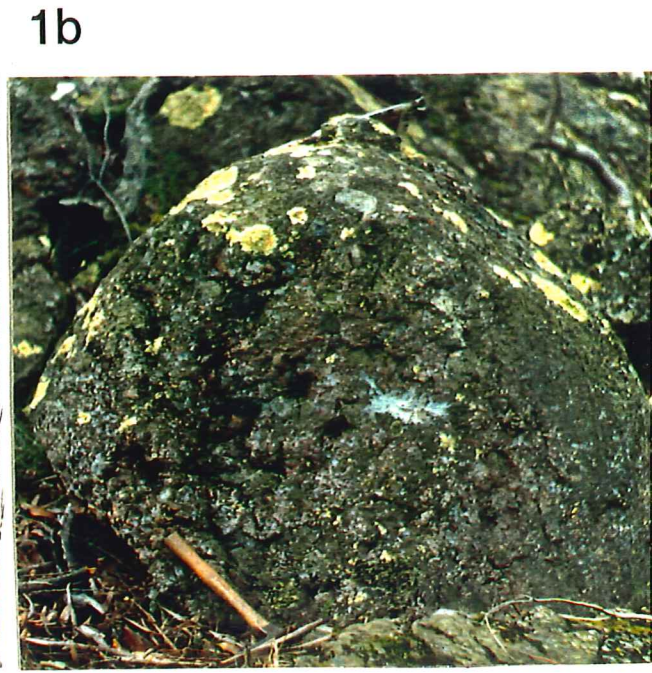
see Appendix 1 for sample and observation locality map

- 1a. Sillimanite gneiss showing strong schistosity  
and jointing.  
Observation locality A
  
- 1b. Coarse grained undeformed pegmatite.  
Observation locality B
  
- 1c. Part of amphibolite dyke.  
Observation locality C.
  
- 1d. Quartz-biotite schist showing strong vertical  
schistosity.  
Observation locality D.

PLATE I



1a



1b



1c



1d

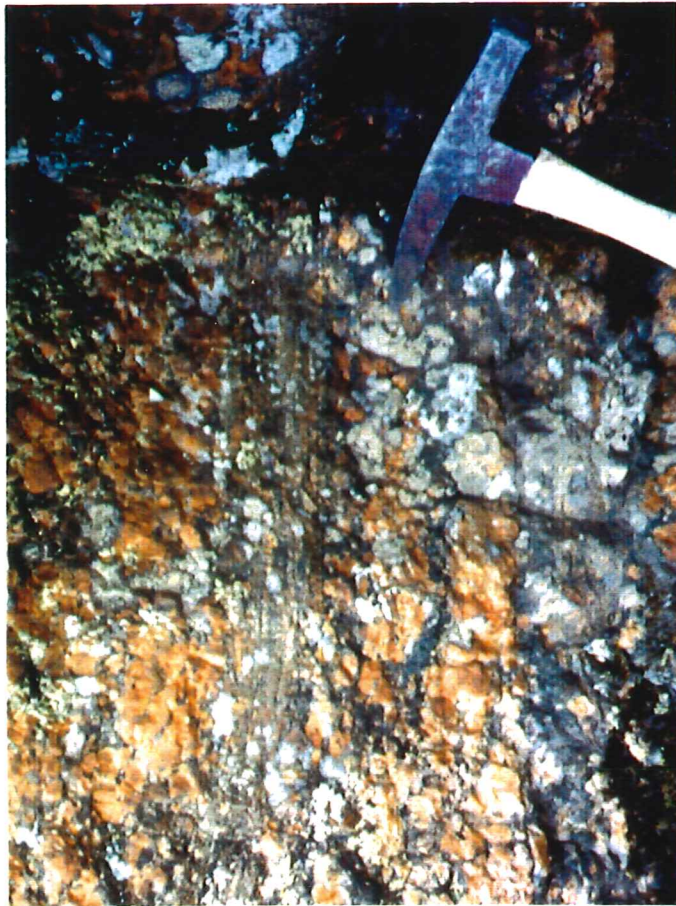


PLATE 2 FIELD PHOTOGRAPHS

see appendix 1 for sample and observation locality map.

- 2a. Coarse grained pegmatite showing shearing running up the photograph.  
Observation locality E.
  
- 2b. Pegmatite has intruded the intensely folded migmatites.  
Observation locality F.
  
- 2c. One coarse grained undeformed pegmatite has intruded an earlier more deformed pegmatite.  
Observation locality G.
  
- 2d. Intensely deformed and migmatized pegmatite.  
Observation locality H.

PLATE 2



2a



2b



2c



2d

## **2.3 Petrography**

### **2.3.1 Gneisses**

#### **(1) Quartz-biotite gneiss**

This common gneissic type shows a reasonably strong lineation of minerals in thin section. The dominant mineral is quartz (40% or more), which are equigranular crystals (0.2-0.5mm) and are clear under plain polarized light (ULP). They exhibit undulose extinction under crossed polars (UXP).

Most of the feldspar has been entirely retrogressed to a fine-grained matrix of sericite, although some relic potassium feldspar with simple twinning and plagioclase remains. Perthitic textures can also be seen. Feldspars constitute at least 40% of the total area of the slide. The crystals are grey and corroded, indicating alteration. The sericite show multiple colours, from grey to high blues (UXP) and very little muscovite could be found.

The biotite usually constitutes only 10-15% of the total thin section although it may rarely be as much as 40%. It appears as elongate crystals with reasonable cleavage with a strong pleochroism from a light fawn colour to a dark brown (UPL). They show high birefringent colours, up to bright greens (UXP) and parallel extinction. The crystals are reasonably equigranular, ranging in size from 0.2-0.5mm. They are commonly corroded and slightly altered on the rims. 1-2% of very dark opaques are present. Electron probe analysis show them to be iron-rich, but Ti-poor, which would indicate magnetite or haematite, rather than ilmenite.

#### **(2) Sillimanite-bearing Gneiss**

This rock is very similar to the above biotite-quartz gneiss, with quartz and feldspar as the dominant components. It does, however, contain two different characteristic minerals. Sillimanite constitutes up to 10% of the total mineral content in some specimens. They are well-shaped crystals with high relief and have a strong preferred orientation. Traversely, they are diamond shaped and exhibit only low colours (UXP). There is a good cleavage, diagonally crossing the crystal (plate 3a ).

Longitudinally the crystals are very elongate, almost fibrous in appearance, showing orthogonal fracturing. They are clear (UPL) and show high colours (UXP). Most are corroded and altered to sericite which surrounds all the crystals. In some places, the sericite has completely replaced the sillimanite, but the relic sillimanite outline is obvious ( plate 3b ).

Garnet is also a characteristic mineral of this rock, but is only present in minor amounts, usually as small fragments of dismembered crystals. They are anhedral and are rimmed by slightly altered biotite and feldspar. Nonetheless, they have high-relief, and are mottled brown (UPL) and isotropic (UXP). The dominant composition indicated by probe analysis is almandine garnet ( plate 3c ).

### (3) Quartzo-feldspathic Gneiss

This gneissic type has a wide range of mineral compositions. It varies from a quartz biotite gneiss as described above, to a pyroxene-plagioclase rich rock. Some thin sections are dominated by 60-70% quartz and have less than 10% biotite content with preferred orientation and subtle segregation features. Most of the feldspar has been replaced by sericite and there are relicts of sillimanite which have also been replaced.

Other specimens contains only 50% quartz and up to 30-40% feldspar, with no biotite. The quartz crystals are large and intergranular. The feldspar is predominantly plagioclase, but is severely altered to sericite. Epidote is a characteristic mineral in this rock, although it is not easily recognizable in hand specimen. It constitutes about 10% of the thin section and appears as small, randomly orientated, fawn to tan-yellow coloured crystals (ie. pleochroic) and shows high colours (UXP) ( plate 3g ).

The other extreme version of the quartzo-feldspathic gneiss contains less quartz (5-10%). It also contains clinopyroxene (diopside) and amphiboles (hornblende). The feldspars are plagioclase (albite) and a minor percentage of opaques are present (Fe-rich, magnetite, haematite). It seems to be a less retrograde metamorphic version of the above sample.

### **2.3.2 Schists**

The schists in thin section are more homogeneous. They are dominated by up to 70% quartz, which appears as equigranular crystals approximately 5mm in size, with very small dusty inclusions. They contain minor feldspar and less mica, dominantly elongate biotite, with muscovite and actinolite which flows around the quartz grains ( plate 3c ).

### **2.3.3 Intrusives**

#### **(1) Amphibolite**

The amphibolite consists predominantly of feldspar and amphiboles. The feldspar is plagioclase, showing simple twinning in crystals of 0.2-0.5mm in size. They appear as white to grey randomly-orientated crystals of an interlocking nature. From probe work, these were classified as labradorite. It constitutes 30% of the thin section but much is strongly corroded and altered.

The amphibole is rather anhedral in shape, suggesting it is most likely the product of altered pyroxene. The crystals vary from pale to dark green, but are not pleochroic.(UXP) they show very mottled low yellows to occasional high colours (plate 3f ). From probe analysis, they appear to lie in the actinolite-tremolite series.

The amphibole makes up more than 60% of the slide, with opaques constituting approximately another 5%. Probe analysis indicates this is essentially ilmenite (appendix 3 ).

#### **(2) Pegmatites**

The pegmatites have very large mineral grains and composition ranges from 20-80% quartz, with feldspars making up the remainder (20-70%), and minor biotite and opaques. The quartz appears as large crystals up to 5mm in size, which show no undulose extinction. The feldspars are smaller and are partly sericitized. Although there is some plagioclase, perthite is predominant. Large crystals showing white albite intergrown with grey potassium feldspar (probably orthoclase), are also present. Textures appear to be either granophyric or mymekitic.

#### **(3) Aplite/Microgranite**

The aplite/microgranite rock consists of approximately 50-60% 1mm size quartz crystals with an interlocking texture and undulose extinction. Feldspars (50-60%), are mostly perthites where plagioclase lamellae have grown within the potassium feldspar. Biotite (5%) and minor amounts of dark brown hornblende, which has a more subtle cleavage, is non-pleochroic and shows low colours (UXP), make up the remainder.

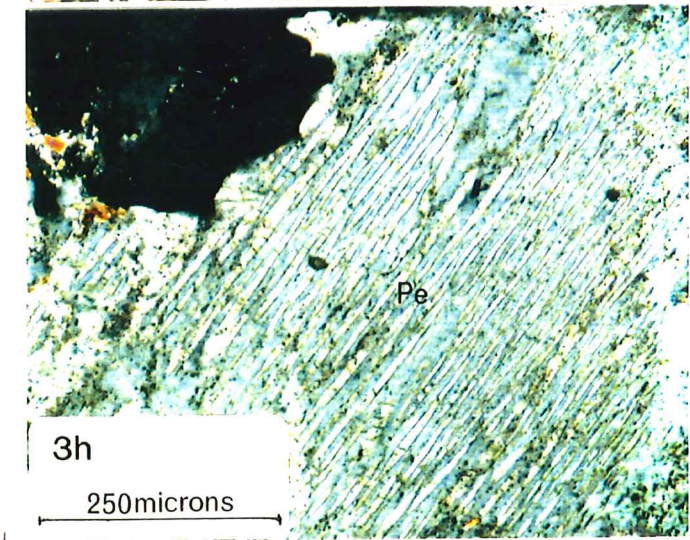
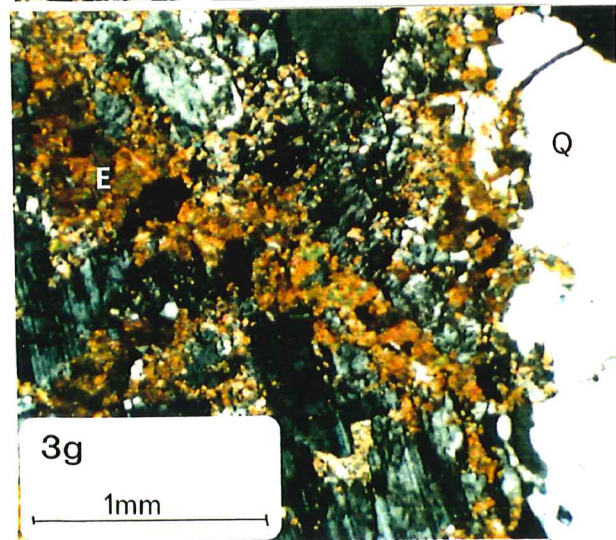
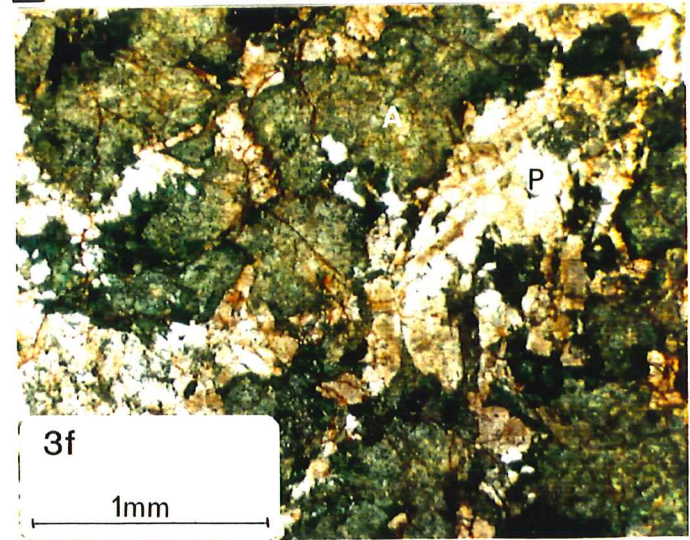
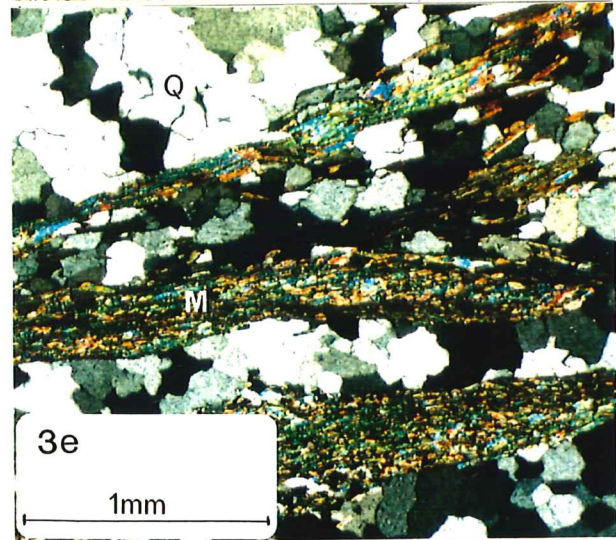
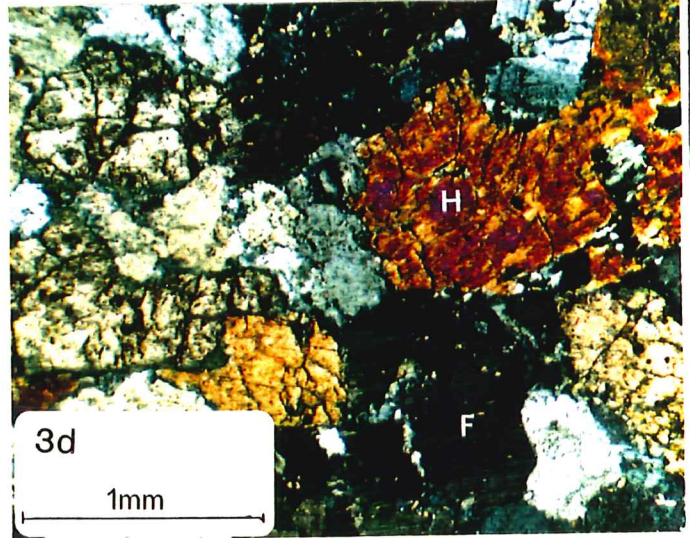
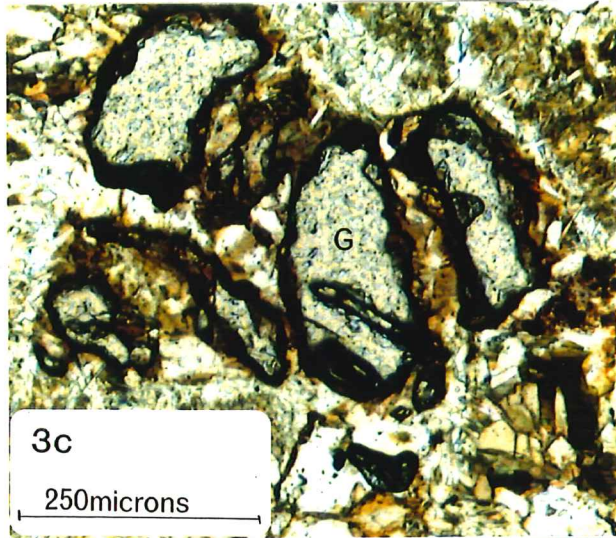
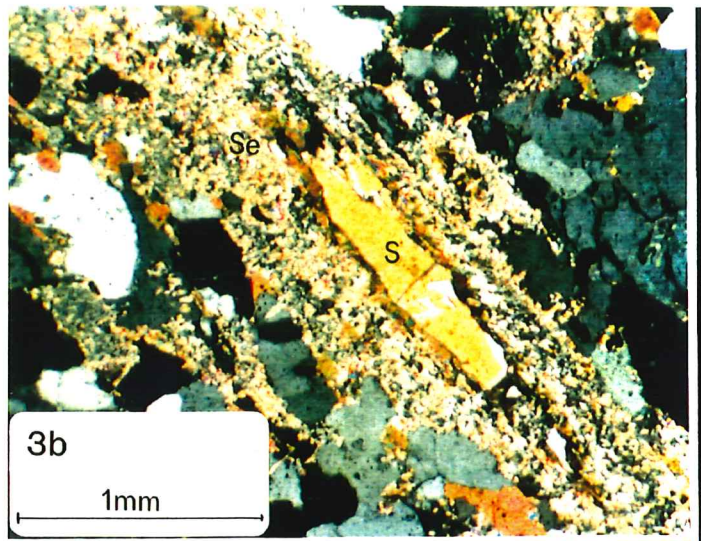
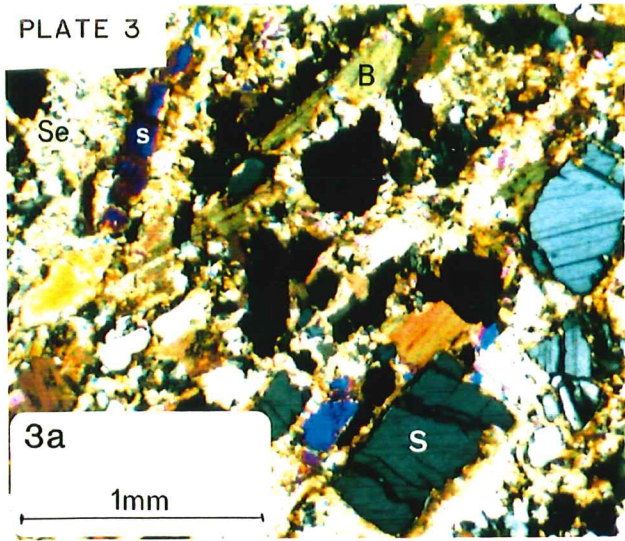
Detailed analysis of the thin sections is found in Appendix 1.

## PHOTOMICROGRAPHS

- 3a & b Sillimanite gneiss showing strong preferred orientation of the crystals and also a lot of alteration.
- 3c. Sillimanite gneiss containing fractured and slightly altered garnets surrounded by sericite and altered biotites
- 3d. Amphibole-pyroxene granulite containing hornblende and various feldspars.
- 3e. Quartz-biotite schist showing strong preferred orientation of the micas.
- 3f. Amphibolite showing plagioclase and altered pyroxenes.
- 3g Quartzo-feldspathic gneiss showing alteration of the plagioclase to epidote.
- 3h. Perthitic textures found in the aplite with plagioclase lamellae in the K-feldspar.

S = Sillimanite  
B = Biotite  
Se = Sericite  
G = Garnet  
H = Hornblende  
F = Feldspar  
Q = Quartz  
E = Epidote  
Pe = Perthite

PLATE 3





### 3. GEOCHEMISTRY

#### 3.1 Introduction

The following chapter discusses results obtained from geochemical analysis of three major lithologies found in the field area. These being the 1) amphibolite, 2) pegmatite and aplite and 3) the 'Houghton' granulite.

#### 3.2 Amphibolite

The amphibolite composition closely resembles the average composition of a gabbro. Table 1 compares its composition with another from an inlier near Normanville ( Davies, 1972 ) and other similar basic rocks. Slight depletion of  $Al_2O_3$  and  $Na_2O$  content and a corresponding enrichment of Fe and Ti suggest that metamorphic fluids may have slightly affected the original composition.

A series of discriminatory diagrams have been used by Pearce and Cann (1973), Pearce *et al.* (1975), Winchester and Floyd (1977), Shervais (1982), Mullen (1983), Holm (1985) and Meschede (1986) to distinguish the environment of formation for basic igneous rocks.

On the Ti vs Zr diagram the amphibolites plot as ocean-floor basalts (OFB on fig. 4 ). On the Ti, Zr, Y ternary diagram, they plot in the OFB field and the low-potassium tholeiite (LKT) field ( fig. 3 ). On the Ti vs Cr diagram the amphibolites plot on the boundary of the OFB and the LKT fields ( fig. 5 ). On the  $SiO_2$  vs  $Zr/TiO_2$  diagram they plot in the sub-alkaline basalt field, ( fig. 6 ) but on the  $Zr/TiO_2$  vs  $Nb/Y$  diagram they plot in a nearby field of andesite/basanite ( fig. 7 ). The V vs Ti diagram finds the amphibolites in the calc-alkaline basalt field (fig. 8).

The ternary diagram of  $TiO_2$ , MnO,  $P_2O_5$  finds them plotting on the boundary of mid-ocean ridge basalts ( MORB ) and the Island-arc tholeiites (IAT) (fig. 9 ). The ternary plot  $TiO_2$ ,  $K_2O$ ,  $P_2O_5$  suggests the amphibolites are OFB ( fig. 10 ). The plot Nb, Zr, Y also indicates a MORB origin for the amphibolites ( fig. 11 ).

The general overall trend suggests fairly strongly that the amphibolites were originally ocean-floor basalt. We do not know how far eastward the Proterozoic inlier block extends so we are unable to ascertain whether continental separation occurred at this time or that the basalts could be "a product of an aborted attempt to generate new sea floor" (Pearce *et al.*, 1975) in this particular region.

### 3.3 Pegmatites and Aplite.

The felsic intrusives in the area are reasonably unaltered and are represented by a large body of pegmatite and a minor intrusion of aplite. Both are quartz and feldspar rich, with high SiO<sub>2</sub> ( 65-80% ), Al<sub>2</sub>O<sub>3</sub> ( 14-15% ), Na<sub>2</sub>O ( 3.8% ) and K<sub>2</sub>O ( 2.6-5.6% ) content: indicative of calc-alkaline granites (Ehlers *et al.*, 1980) The Log Rb vs Log Y + Nb discriminatory diagram (Pearce, 1984), is used to distinguish the environment of formation of granitic rocks ( fig. 12 ). This diagram indicates the aplites plot generally in two fields: as either a volcanic arc granite or a within-plate granite.

### 3.4 The 'Houghton' granulite.

As discussed in earlier chapters, there has been considerable debate over whether this rock type ( eg. Benson- diorite and Spry- Ca-rich sandstone ), is igneous or sedimentary in origin.

It occurs in the field as highly metamorphosed bands within the gneissic terrain. This would indicate either a sedimentary bed, or premetamorphic dyke precursor. The average composition of five samples from the field area samples are listed with other analysis by Davies (1972), Spry (1951), Mawson (1926) and Benson (1909) on the 'Houghton' granulite from different inliers. They are compared with other diorites and sedimentary rocks from other sources.

Looking at each analysis by the various authors (Table 2.) the 'Houghton' granulite shows a regional compositional variation. Apart from some enrichment in Fe<sub>2</sub>O<sub>3</sub> and depletion in CaO, the average field sample closely resembles Alderman

(1938) and Benson's (1909) analyses. Relative to Spry's (1951) analysis the field samples are depleted in  $\text{SiO}_2$  and  $\text{K}_2\text{O}$ , but enriched in  $\text{Fe}_2\text{O}_3$  and  $\text{Na}_2\text{O}$ .

This variation of composition between individual samples of the same rock type may be due to inaccuracies in the geochemical analysis or metamorphic alteration. Therefore, on a geochemical basis, it makes comparisons to other rock types not entirely conclusive. Relative to basic diorites, the granulite is enriched in Fe,  $\text{Na}_2\text{O}$  and Rb and depleted in CaO, MnO and Sr. In comparison to sediments the granulite is enriched in Fe and  $\text{Na}_2\text{O}$  and depleted in CaO. Of the sediments, the granulite closely resembles a shale.

Considering the age of the rock and the metamorphic alteration that has occurred, the origin of the granulite is a matter of conjecture, but overall, the granulite closely resembles a diorite composition.

### 3.5 Discussion

The Harker diagrams in figure 13 seem to show the usual trend of depletion of many major and trace elements when moving from mafic to felsic rocks. Exceptions to this include  $\text{Al}_2\text{O}_3$ ,  $\text{Na}_2\text{O}$ , Rb, Nb, Y and La, where the trend is the opposite.

This may be due to the concentration of the large ion lithophile elements ( Nb, Y, La ) in the more felsic melts. The high concentrations of  $\text{Al}_2\text{O}_3$  and  $\text{Na}_2\text{O}$  in the felsic rocks is affected by the large content of feldspar.

The pegmatites have higher Cr and Zr contents than the aplite occurring during differentiation of wet and dry fluids.

The granulite has a similar  $\text{SiO}_2$  content ( 58.84-61.99 %) in all five samples, but internal variation of other elements is quite large, compared to the good grouping of the other rock types. This may be due to metamorphic alteration or because the original rock was an inhomogeneous mixture of two different rock types with similar silica content.

TABLE 1 : AMPHIBOLITE. Column 1 is the whole rock analysis and column 2 is the enrichment /depletion of the amphibolite with respect to other similar basic rocks.

|                                | A1    | FHG   | CG   | CR    | A2   |       |      |       |      |
|--------------------------------|-------|-------|------|-------|------|-------|------|-------|------|
| SiO <sub>2</sub>               | 50.54 | 53.36 | 0.95 | 50.41 | 1    | 50.41 | 1    | 52.96 | 0.95 |
| Al <sub>2</sub> O <sub>3</sub> | 13.08 | 17.72 | 0.74 | 18.3  | 0.71 | 16.04 | 0.82 | 12.9  | 1.02 |
| Fe <sub>2</sub> O <sub>3</sub> | 15.63 | 7.92  | 1.97 | 10.09 | 1.5  | 8.21  | 1.9  | 12.77 | 1.22 |
| MnO                            | 0.25  | 0.16  | 1.56 | 0.16  | 1.56 | 0.11  | 2.27 | 0.12  | 2.08 |
| MgO                            | 5.99  | 6.6   | 0.91 | 4.25  | 1.41 | 9.47  | 0.63 | 4.15  | 1.44 |
| CaO                            | 9.71  | 8.87  | 1.09 | 11.2  | 0.87 | 11.41 | 0.85 | 7.31  | 1.33 |
| Na <sub>2</sub> O              | 2.23  | 3.3   | 0.68 | 2.74  | 0.81 | 2.31  | 0.97 | 4.06  | 0.55 |
| K <sub>2</sub> O               | 0.48  | 0.62  | 0.77 | 0.46  | 1.04 | 1.15  | 0.42 | 2.22  | 0.22 |
| TiO <sub>2</sub>               | 1.74  | 0.74  | 2.35 | 1.75  | 0.99 | 0.44  | 3.95 | 2.52  | 0.69 |
| P <sub>2</sub> O <sub>5</sub>  | 0.19  | 0.12  | 1.58 | 0.25  | 0.76 | 0.04  | 4.75 | 0.45  | 0.42 |
| Sr                             | 157   | 1565  | 0.1  |       |      | 538   | 0.29 | 95    | 1.6  |
| Rb                             | 19.7  | 268   | 0.07 |       |      | 37    | 0.53 | 38    | 0.52 |
| Y                              | 42    |       |      |       |      | 10.3  | 4.08 |       |      |
| Ba                             | 388   | 1100  | 0.35 |       |      | 2452  | 0.16 | 166   | 2.38 |
| Sc                             | 4     |       |      |       |      | 41    | 0.1  |       |      |
| Ni                             | 49    |       |      |       |      | 122   | 0.4  | 31    | 1.58 |
| V                              | 392   | 200   | 1.96 |       |      | 197   | 2    | 552   | 0.78 |
| Cr                             | 51    | 10    | 5.1  |       |      | 157   | 0.32 | 12    | 4.25 |
| Ga                             | 22    |       |      |       |      | 15    | 1.46 |       |      |
| Ce                             | 37    |       |      |       |      | 25    | 1.48 | 141   | 0.26 |
| Nd                             | 25    |       |      |       |      | 3     | 8.33 |       |      |
| La                             | 19    |       |      |       |      | 11    | 1.73 | 141   | 0.13 |
| Zr                             | 117   | 200   | 0.59 |       |      | 45    | 2.6  |       |      |
| Nb                             | 10.7  |       |      |       |      | 2.4   | 4.46 |       |      |

A1 = average of amphibolite analysis from field area.

FHG = Foliated-hypersthene gabbro from Moore et al (1979).

OG = Olivine-gabbro from Moore et al (1979).

OR = Orthogabbro from Sando (1987).

A2 = Amphibolite from Normanville Inlier ( Davies,1972).

TABLE 2: 'HOUGHTON' GRANULITE. Column 1 is the rock analysis and column 2 is the enrichment /depletion of the granulite with respect to some basic diorites and sedimentary rocks.

|                                | HG    | D1    | D2   | HG2   | HG3  | HG4   | HG5  | LO    | SH1  | GR    | SH2  | SE*   |      |       |      |       |      |      |      |       |      |       |      |
|--------------------------------|-------|-------|------|-------|------|-------|------|-------|------|-------|------|-------|------|-------|------|-------|------|------|------|-------|------|-------|------|
| SiO <sub>2</sub>               | 59.48 | 59.17 | 1.01 | 55.77 | 1.07 | 54.15 | 1.09 | 69.25 | 0.86 | 58.19 | 1.02 | 56.85 | 1.05 | 64.61 | 0.92 | 55.43 | 1.07 | 64.7 | 0.92 | 61.75 | 0.96 | 57.95 | 1.03 |
| Al <sub>2</sub> O <sub>3</sub> | 14.65 | 16.41 | 0.89 | 17.25 | 0.84 | 15.78 | 0.93 | 13.4  | 1.09 | 15.28 | 0.96 | 14.76 | 0.99 | 10.64 | 1.38 | 15.4  | 0.95 | 14.8 | 0.99 | 14.5  | 1.01 | 13.39 | 1.1  |
| Fe <sub>2</sub> O <sub>3</sub> | 9.85  | 6.84  | 1.44 | 6.69  | 1.47 | 6.06  | 1.63 | 4.16  | 2.36 | 3.81  | 2.6  | 5.69  | 1.73 | 3.11  | 3.17 | 5.74  | 1.72 | 5.4  | 1.82 | 7.81  | 1.26 | 5.55  | 1.77 |
| MnO                            | 0.02  | 0.13  | 0.15 | 0.12  | 0.17 | 0.29  | 0.07 | 0.01  | 0.5  | 0.05  | 0.4  | 0.12  | 0.17 | 0.05  | 0.4  |       |      | 0.1  | 0.2  | 0.12  | 0.17 |       |      |
| MgO                            | 2.85  | 3.72  | 0.77 | 5.6   | 0.51 | 2.23  | 1.28 | 1.53  | 1.9  | 3.85  | 0.74 | 3.89  | 0.73 | 3.69  | 0.77 | 2.67  | 1.06 | 2.2  | 1.29 | 2.6   | 1.11 | 2.65  | 1.08 |
| CaO                            | 2.67  | 6.16  | 0.43 | 7.54  | 0.35 | 10.58 | 0.25 | 2.47  | 1.08 | 8.72  | 0.31 | 7.41  | 0.34 | 5.41  | 0.49 | 5.96  | 0.45 | 3.1  | 0.86 | 1.2   | 2.2  | 5.89  | 0.45 |
| Na <sub>2</sub> O              | 6.27  | 3.84  | 1.6  | 5.36  | 1.17 | 0.83  | 7.55 | 3.03  | 2.07 | 4.76  | 1.32 | 5.34  | 1.17 | 1.35  | 4.64 | 1.8   | 3.48 | 3.1  | 2.02 | 0.8   | 7.8  | 1.13  | 5.55 |
| K <sub>2</sub> O               | 2.92  | 1.58  | 1.85 | 0.89  | 3.28 | 4.9   | 0.06 | 4.66  | 0.63 | 3.02  | 0.97 | 1.91  | 1.53 | 2.06  | 1.42 | 2.67  | 1.09 | 1.9  | 1.54 | 4.24  | 0.69 | 2.86  | 1.02 |
| TiO <sub>2</sub>               | 0.54  | 0.93  | 0.58 | 0.48  | 1.13 | 0.64  | 0.84 | 0.91  | 0.59 | 2.65  | 0.2  | 3.11  | 0.17 | 0.4   | 1.35 | 0.46  | 1.17 | 0.5  | 1.08 | 0.72  | 0.75 | 0.57  | 0.95 |
| P <sub>2</sub> O <sub>5</sub>  | 0.16  | 0.24  | 0.67 | 0.13  | 1.23 | 0.17  | 0.94 | 0.13  | 1.23 | 0.48  | 0.3  | 0.51  | 0.3  | 0.06  | 2.67 | 0.2   | 0.8  | 0.2  | 0.8  | 0.05  | 3.2  | 0.13  | 1.23 |
| Sr                             | 55    | 1000  | 0.06 | 431   | 0.12 | 263   | 0.21 |       |      |       |      |       |      |       |      |       |      |      |      |       |      |       |      |
| Pb                             | 59    | 22    | 2.68 | 31    | 1.9  | 283   | 0.21 |       |      |       |      |       |      |       |      |       |      |      |      | 17    | 3.11 |       |      |
| Y                              | 53    | 50    | 1.06 | 12.4  | 4.3  |       |      |       |      |       |      |       |      |       |      |       |      |      |      | 210   | 1    |       |      |
| Ba                             | 210   | 50    | 4.2  | 231   | 0.91 | 864   | 0.24 |       |      |       |      |       |      |       |      |       |      |      |      |       |      |       |      |
| Sc                             | 15    |       |      | 26.1  | 0.57 |       |      |       |      |       |      |       |      |       |      |       |      |      |      |       |      |       |      |
| Ni                             | 21    | 30    | 0.7  | 76    | 0.28 | 55    | 0.38 |       |      |       |      |       |      |       |      |       |      |      |      |       |      |       |      |
| V                              | 83    | 200   | 0.42 | 185   | 0.45 | 69    | 1.2  |       |      |       |      |       |      |       |      |       |      |      |      |       |      |       |      |
| Cr                             | 55    | 75    | 0.73 | 144   | 0.38 | 92    | 0.6  |       |      |       |      |       |      |       |      |       |      |      |      |       |      |       |      |
| Ga                             | 25    |       |      | 18    | 1.39 |       |      |       |      |       |      |       |      |       |      |       |      |      |      |       |      |       |      |
| Ce                             | 78    |       |      | 35    | 2.2  | 125   | 0.62 |       |      |       |      |       |      |       |      |       |      |      |      | 65    | 1.2  |       |      |
| Nd                             | 49    |       |      | 19    | 2.58 |       |      |       |      |       |      |       |      |       |      |       |      |      |      | 23    | 2.1  |       |      |
| La                             | 35    |       |      | 21    | 1.67 | 25    | 1.4  |       |      |       |      |       |      |       |      |       |      |      |      | 29    | 1.2  |       |      |
| Zr                             | 133   | 200   | 0.67 | 77    | 1.73 |       |      |       |      |       |      |       |      |       |      |       |      |      |      |       |      |       |      |
| Nb                             | 7.5   |       |      | 2.3   | 3.26 |       |      |       |      |       |      |       |      |       |      |       |      |      |      |       |      |       |      |

HG = average of 'Houghton' granulite analysis from the field area.

D1 = Diorite from Moore et al (1979)

D2 = Diorite from Sando (1987)

HG2 = 'Houghton' granulite from Normanville Inlier (Davies, 1972).

HG3 = Analysis of 'Houghton' granulite by Spry (1951)

HG4 = Analysis of 'Houghton' granulite by Alderman (1938).

HG5 = Analysis of 'Houghton' granulite by Benson (1909).

Fe<sub>2</sub>O<sub>3</sub>\* = Total Fe content.

LO = Loess analysis from Pettijohn (1957).

SH1 = Shale analysis from Pettijohn (1957).

GR = Average greywacke from Pettijohn (1957).

SH2 = Shale from Nance and Taylor (1976).

Se\* = Shale from Pettijohn (1957).

\* Sediment consists of shale 82%, sandstone 12% and limestone 6%.

FIGURE 3. Discrimination diagram from Pearce and Cann (1973) showing the amphibolite plotting in the calc-alkaline basalt and low potassium tholeiite field.

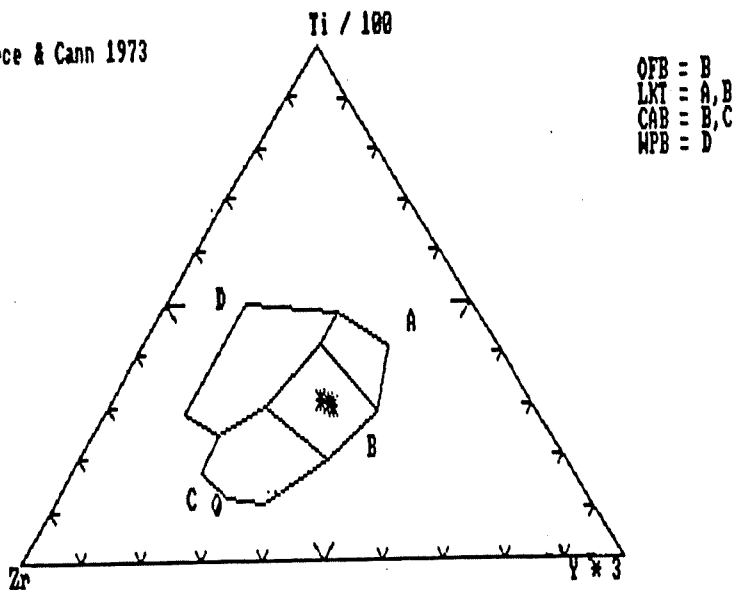
FIGURE 4. Another discrimination diagram from Pearce and Cann (1973) showing the amphibolite plotting in the ocean floor basalt field.

FIGURE 5 Discrimination diagram from Pearce.(1975) showing the amphibolite plotting on the boundary of the low potassium tholeiite field and the ocean floor basalt field.

OFB = ocean floor basalt  
LKT = low potassium tholeiite  
CAB = calc-alkaline basalt  
WPB = within plate basalt

**FIGURE 3**

Pearce & Cann 1973



**FIGURE 4**

Pearce & Cann 1973

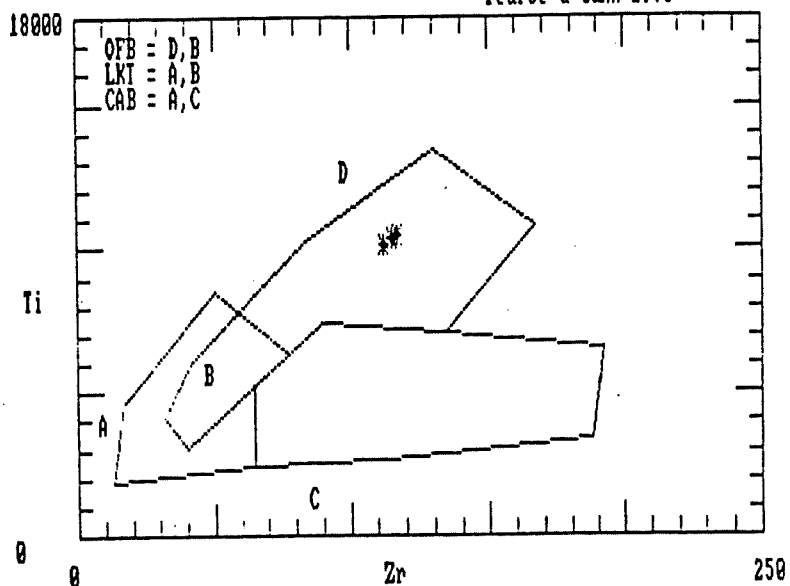


**FIGURE 5**

Pearce 1975

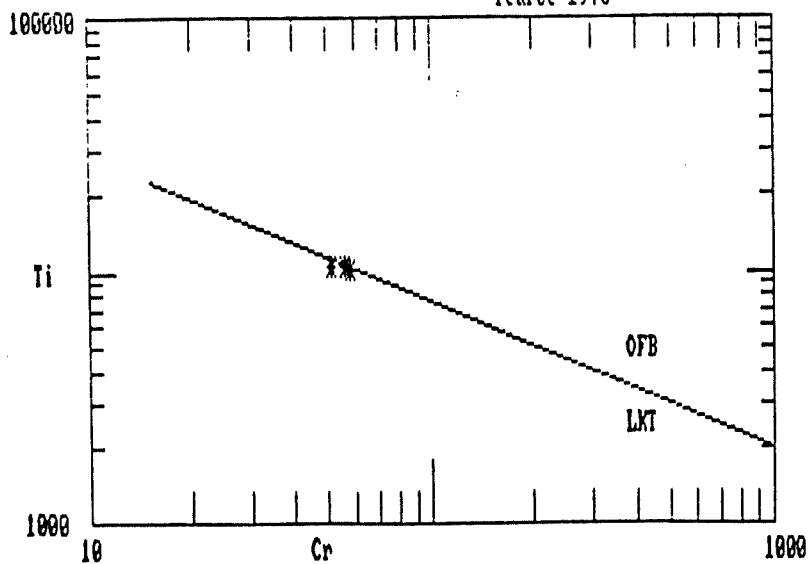


FIGURE 6. Discrimination diagram from Winchester and Floyd (1977) showing the amphibolite plotting in the andesite/basanite field.

FIGURE 7. Discrimination diagram from Winchester and Floyd (1977) showing the amphibolite plotting in the sub-alkali basalt field.

FIGURE 8. Discrimination diagram from Shervais (1982) showing the amphibolite plotting in the calc-alkaline basalt field.

\* = amphibolite

Rhy = Rhyolite

Rhy/Dac = Rhyo-dacite

And = Andesite

Sab = Sub-alkali basalt

AB = Aluminous basalt

Phon = Phonolite

Tr/An = Trachy-andesite

Tr = Trachyte

CAB = Calc-alkaline basalt



**FIGURE 6**

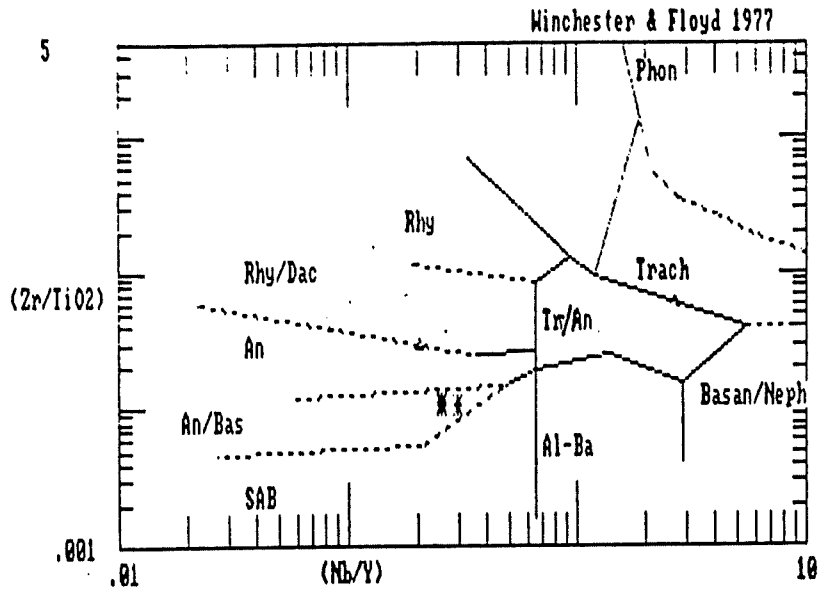


**FIGURE 7**

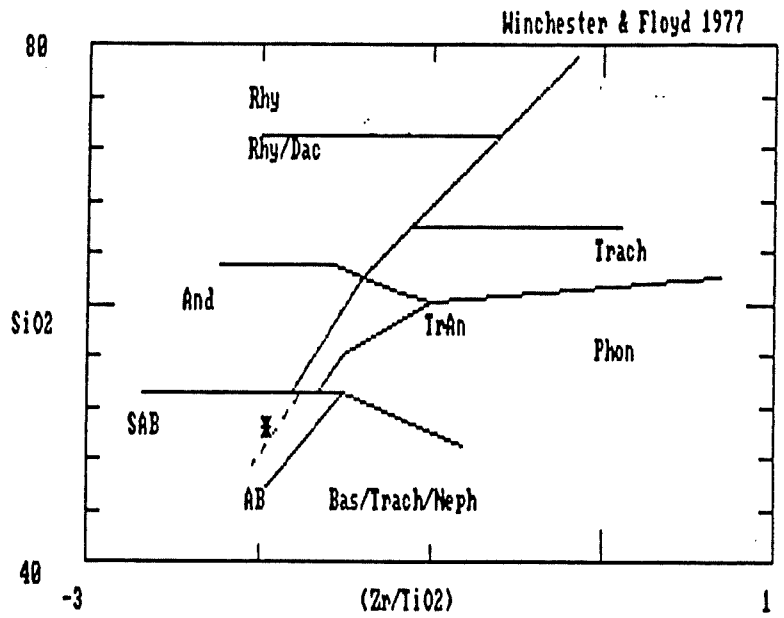


**FIGURE 8**

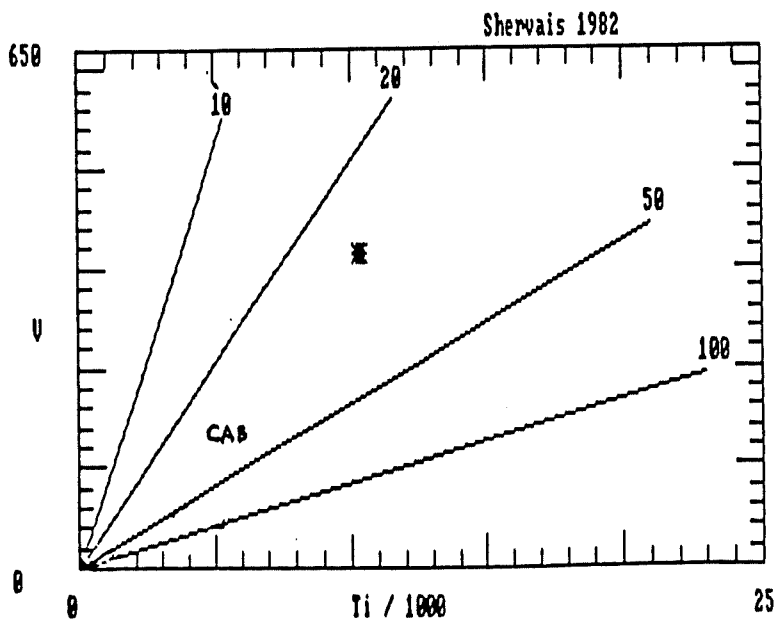


FIGURE 9            Discrimination diagram from Mullen (1983) showing the amphibolite plotting in the mid-ocean ridge basalt field.

FIGURE 10          Ternary diagram TiO<sub>2</sub>-K<sub>2</sub>O-P<sub>2</sub>O<sub>5</sub> from Holm (1985) showing the amphibolite plotting in the ocean floor basalt field.

FIGURE 11          Discrimination diagram from Meschede (1986) showing the amphibolite plotting in the mid-ocean ridge basalt field.

\* = amphibolite

MORB = mid-ocean ridge basalt

OIT = ocean island tholeiite

OIA = ocean island andesite

IAT = island-arc tholeiite

CAB = calc-alkaline basalt

OT = oceanic tholeiite

WPA = within plate andesites

WPT = within plate tholeiite

VAB = volcanic-arc basalt

**FIGURE 9**

Mullen 1983

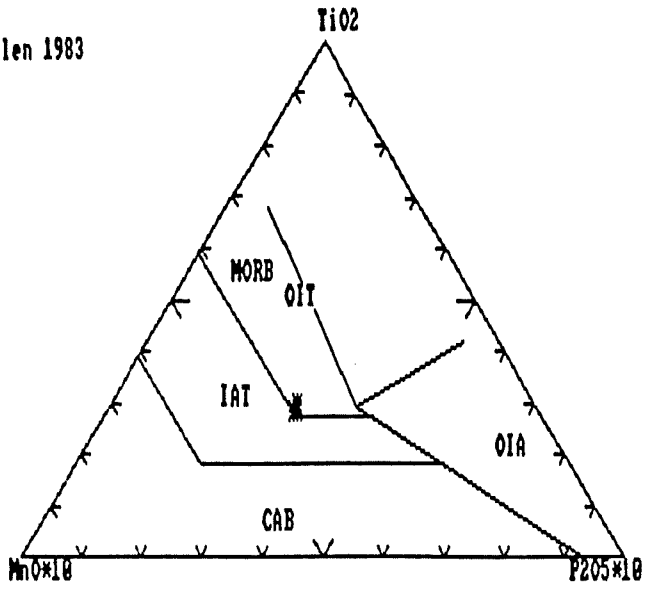


**FIGURE 10**

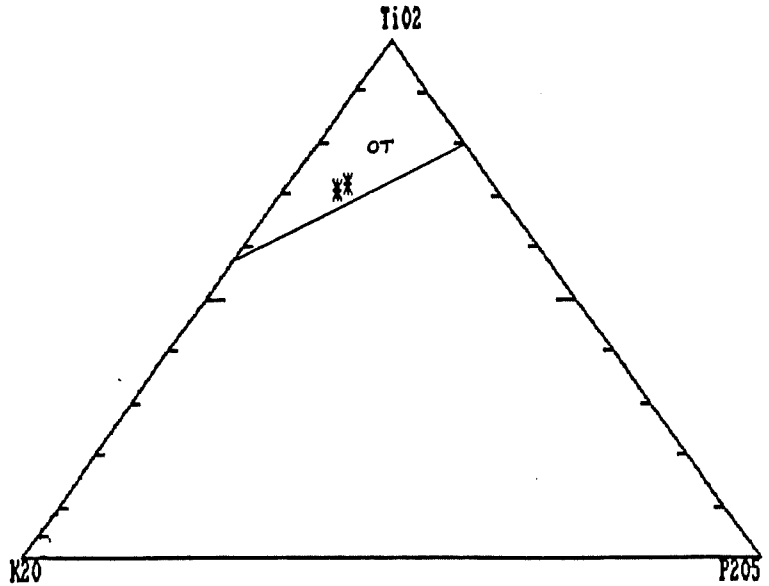


**FIGURE 11**

Meschede 1986

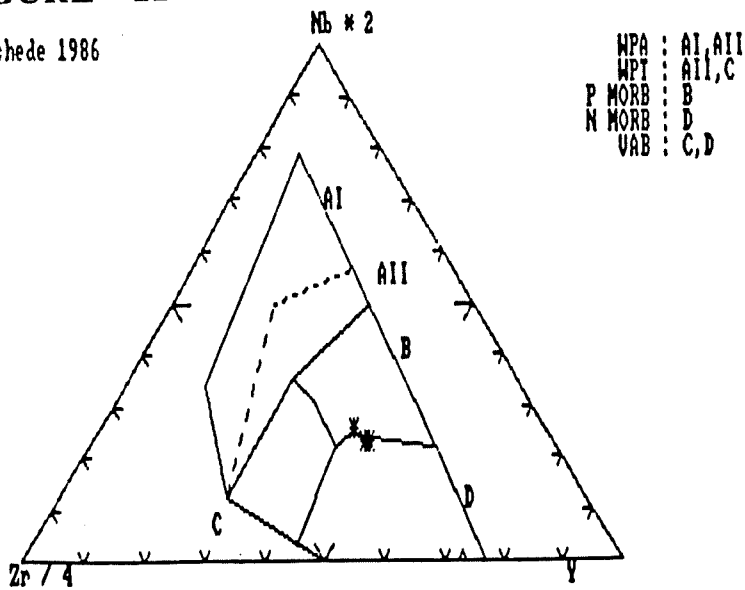


FIGURE 12. Discrimination diagram from Pearce (1984) showing the aplite and the pegmatite plotting in the within plate granite and volcanic arc granite fields.

syn-COLG = syn-collisional granite  
WPG = within plate granite  
VAG = volcanic arc granite  
ORG = orogenic granit

FIGURE 13. Harker diagrams

\* = amphibolite  
 $\Delta$  = 'Houghton' granulite  
 $\square$  = pegmatite  
 $\bullet$  = aplite

FIGURE 13

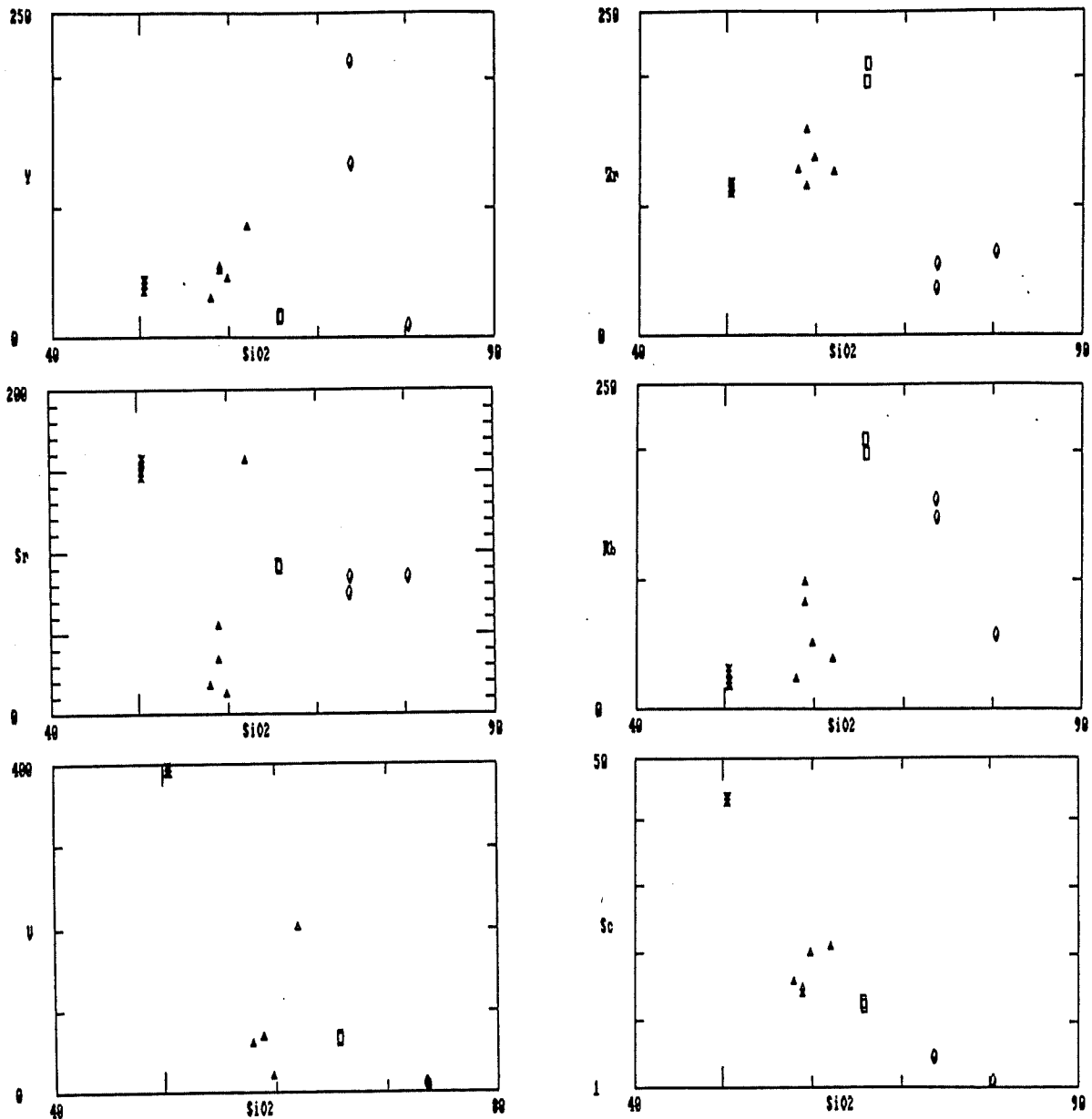


FIGURE 12

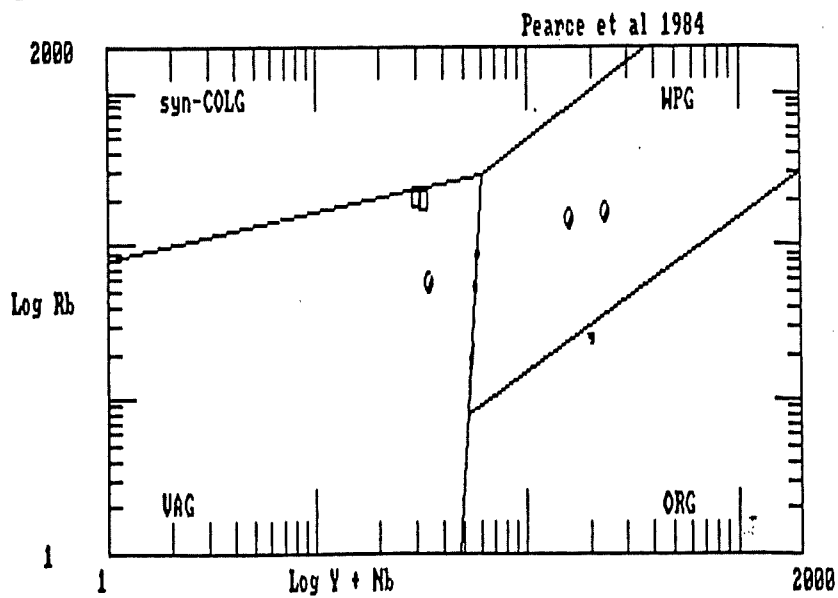
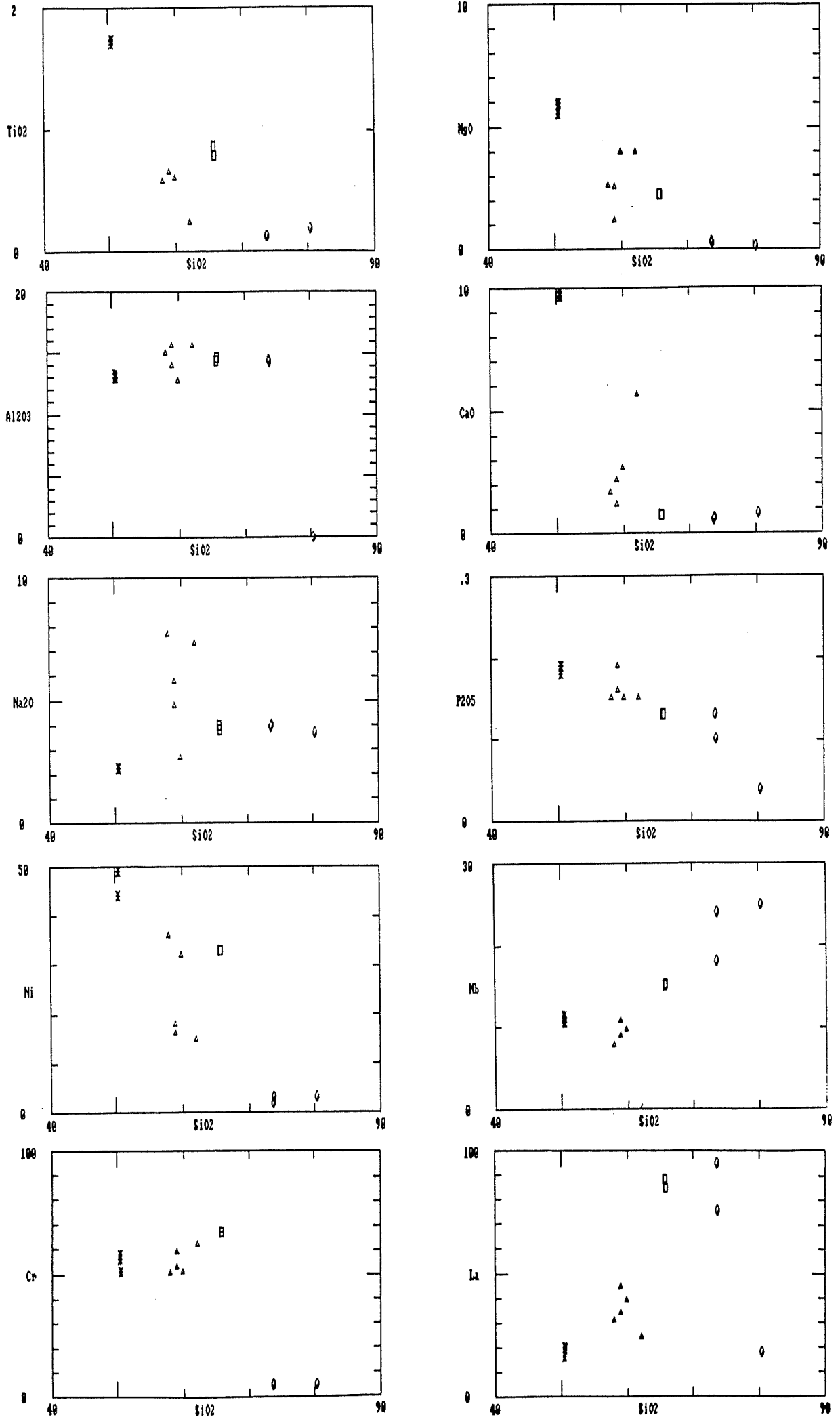


FIGURE 13



## 4. STRUCTURE AND METAMORPHISM

### 4.1 Structure

Previous authors (Spry, 1951 ; McEwin, 1972) have recognized three phases of folding in the Myponga-Yankalilla Inlier; the first two being in the Proterozoic and the third, during the lower Palaeozoic Delamerian Orogeny. During the Palaeozoic, or closely thereafter, a tectonic thrust was formed on the western limb of the anticline. The eastern limb is lost deep under Permian and more recent sediments.

My field observations indicate a slightly more complex folding history. An original metamorphic event, which was of upper amphibolite facies, produced a preferential gneissic layering known as S1, but there is no recognized folding (F1).

S1 could have formed during burial and compaction of the original sedimentary pile and may parallel the original S0 bedding.

F2 folding has been recognized in the gneisses as the very tight to isoclinal folding which have a distinct axial planar foliation, S2. This, in most cases, overprints the near parallel S1 fabric and generally trends E-W, with the inclined limbs dipping north ( plate 4a-d and fig 18).

A strong orthogonal schistosity pattern is observed where an S3 schistosity cuts the S2 fabric in the gneissic rocks, which has one recognizable associated large scale fold (F3) that has a north trending axis.

The final deformation (D4) occurred under retrograde greenschist metamorphism and is recognized in the basement rocks as the distinct, near vertical schistosity that is prominent in the schists, and trends 060N.

The timing of the intrusives in the area is partially restricted by the deformation history. The amphibolite dyke and the aplite intrusion are probably post-D2 because they are not intensely folded. The dyke is pre-D4 because of its amphibolite grade metamorphism.

The migmatites are most probably a product of the original high grade metamorphism when partial melting occurred. This, along with evidence of intense folding, indicate they are a pre-D2 feature.

The pegmatites can be classified into two groups. The older pegmatites show signs of major deformation as intense shear zones. (Plate 2a ). The older pegmatites and migmatites are intruded by a younger pegmatite which cuts across the previous features and shows no sign of major shear zone deformation. (Plate No. 2b ) It is likely all the pegmatites intruded post-D2 deformation, as post-tectonic intrusives; similarly with the aplite and amphibolite.

Besides the relatively minor shear zones, evidence of faulting can be seen in the steep E-W trending valleys and the E-W trending jointing pattern in the gneisses in the field area, which may have been formed by vertical block faulting. Parkin (1969) suggests a Tertiary tectonic event of block faulting and uplift have produced the relief seen in the Mt.Lofty Ranges today.

To the east of the field area, there can be found a heavily weathered lateritic horizon. These Quarternary deposits are remnants of the uplifted terrain ( Parkin, 1969). Offler and Fleming (1968) suggest that the final deformation/folding event seen in the basement, is seen in the cover rocks, where it is called F1. They have recognized folds up to F4 in the cover which are not recognized in the basement.



PLATE 4 FIELD PHOTOGRAPHS

see appendix 1 for sample and observation locality map.

4a - 4d. The intense tight to isoclinal folding can be seen in the Quartz-biotite gneiss.

4a. Observation locality I.

4b. Observation locality J.

4c. Observation locality K.

4d. Observation locality L.

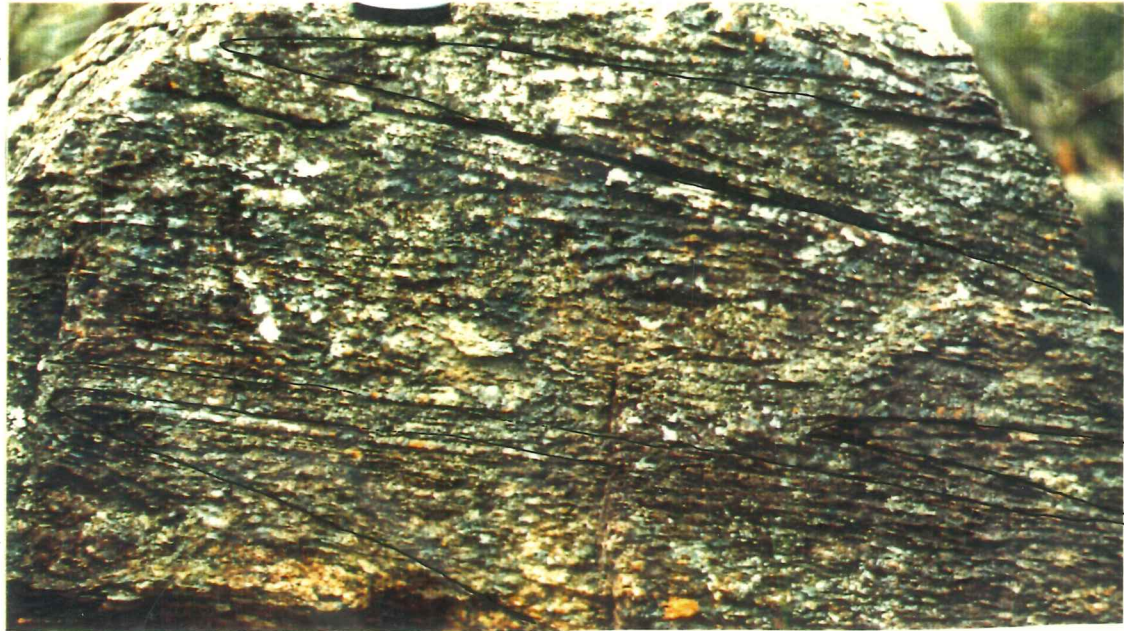
4a



4b



4c



4d



## 4.2 Metamorphism

The rocks in the area are dominated by metamorphic pelites of the amphibolite facies, which consist of micaceous schists and gneisses. Also, feldspathic sandstones have converted to quartzo-feldspathic schists and gneisses and the basalts/andesites to amphibolites. Metamorphic pelites indicate a mudstone/claystone as the original sedimentary rock. The typical amphibolite facies mineralogy, which have a pelite as a precursor rock are garnet, biotite, muscovite, feldspar, sillimanite and quartz (Ehlers & Blatt, 1980) ( See figure 15; ternary diagrams ).

Under high grade metamorphism (650-700°C) the original muscovite has broken down and been altered to K-feldspar (Winkler, 1965).

The occurrence of migmatites in the area suggests that anatexis in the gneisses was reached, also defining the boundary of high-grade metamorphism (if  $P_{H_2O}$  is larger than 3.5kb)( Winkler, 1965).

The common occurrence of sillimanite in the gneisses serves as a temperature indicator. At high temperatures andalusite and cordierite are replaced by almandine and sillimanite.

Many of the pelitic rocks contain perthitic textures, where K-feldspar commonly has plagioclase lamellae. This feature is considered to be of exsolution origin, although replacement can occur ( Hubbard, 1965). This indicates the feldspars must have reached temperatures above the solvus before cooling ( i.e. >680°C ), which implies at least upper amphibolite facies. ( Ehlers and Blatt,1980 ) ( fig. 14 ).

Retrograde metamorphism in the map area is indicated by the abundance of schists, which are retrograde products of a gneiss developed step-by-step under a shearing action. The augen textures in the schists indicate a halfway process. The schists are a retrograde trend towards a fine grained more schistose rock with all high grade minerals retrograded (Spry, 1951 ).

The common retrograde minerals recognized include epidote, amphiboles and sericite, which indicates a retrogradation to greenschist facies. Sillimanite, muscovite and probably plagioclase have been altered to sericite; calcic-plagioclase to epidote.

The amphiboles, hornblende and actinolite, are formed by the breakdown of the unstable clinopyroxene, remnants of which are recognized in the amphibolite dyke. This indicates that the present dyke outcrop was emplaced as a dry magma at depth and was amphibolitized by metamorphic fluids.

Pressure-temperature conditions during shearing are therefore lower than the earlier metamorphism. This suggests a change in depth of burial i.e. some cover removal before shearing.

The evidence indicates that the Proterozoic Inlier rocks, now partially retrograde to greenschist facies, have been at least of upper amphibolite facies grade.

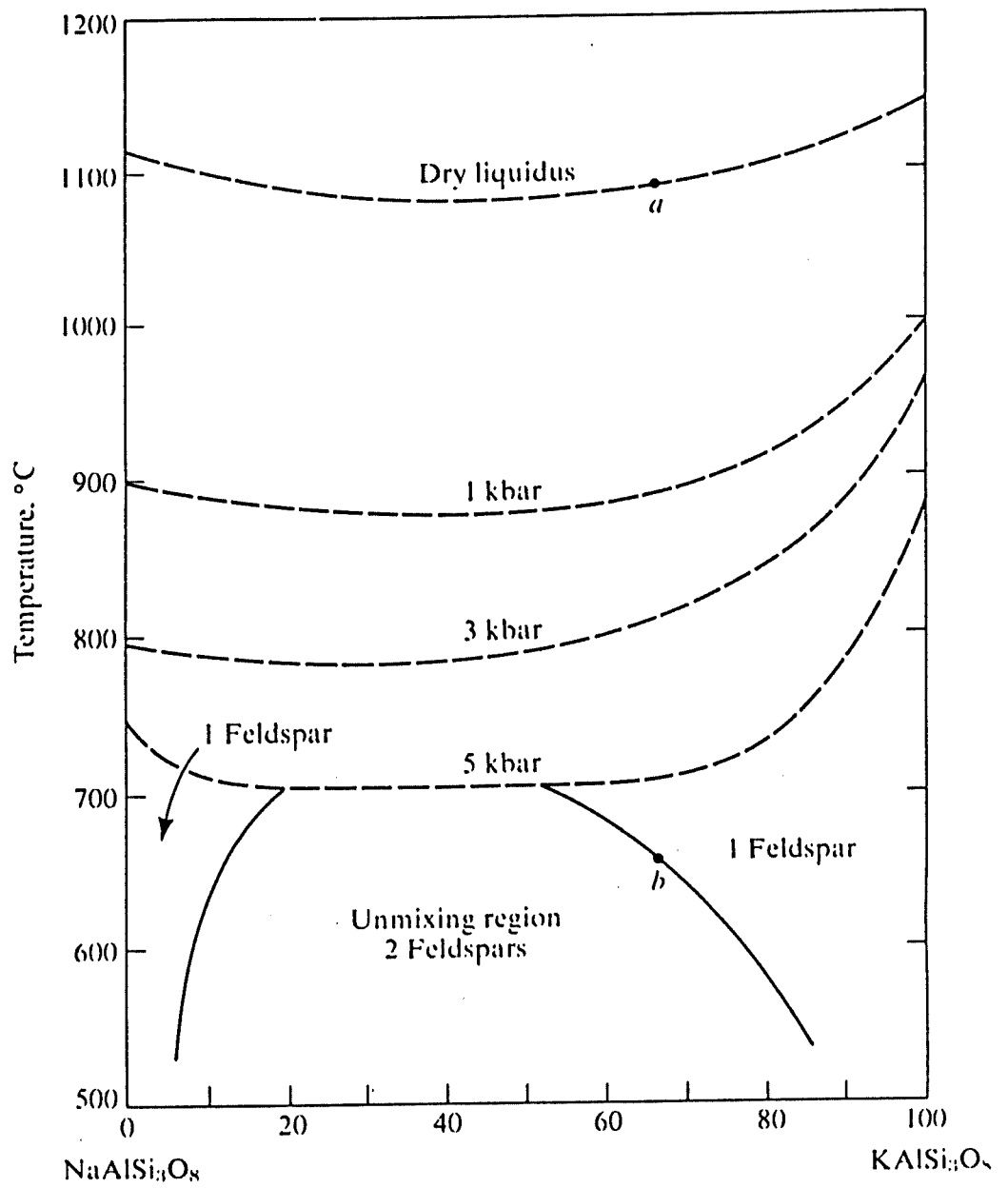
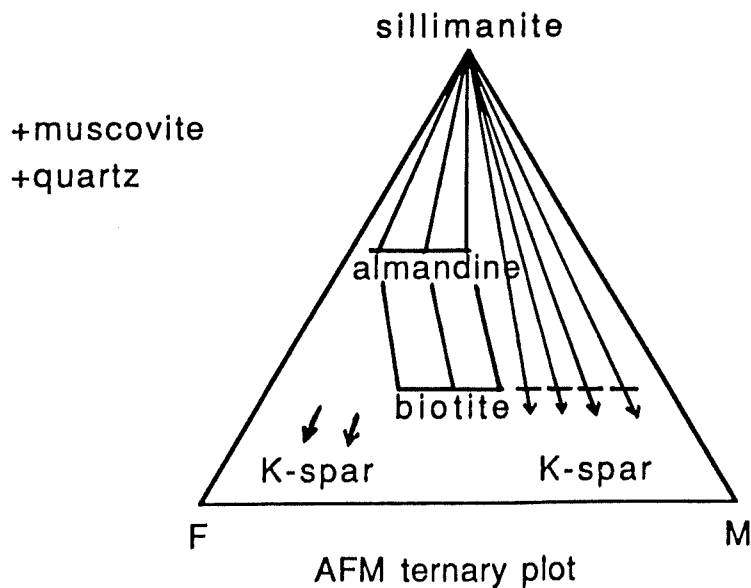
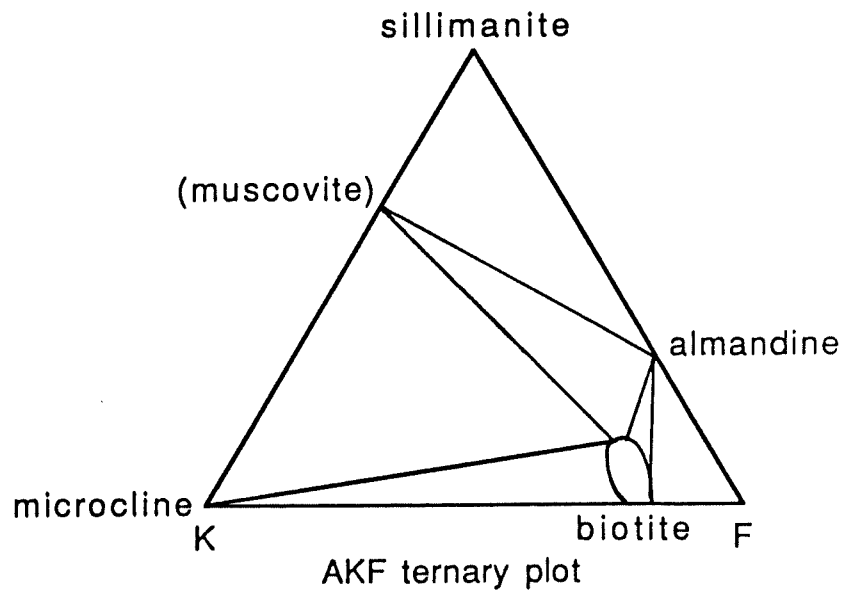
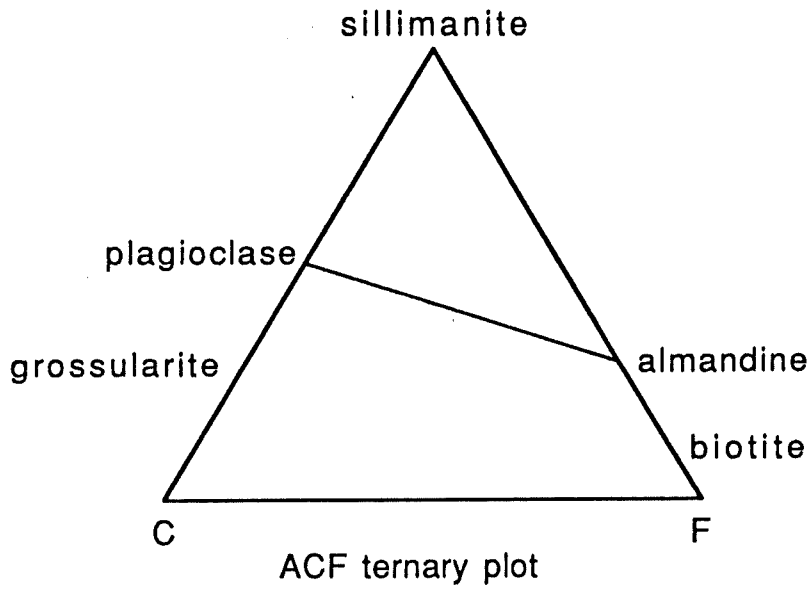


**FIGURE 14**  
 The system NaAlSi<sub>3</sub>O<sub>8</sub>-KAlSi<sub>3</sub>O<sub>8</sub>-H<sub>2</sub>O.

Figure 15.

Ternary diagrams showing the mineral assemblage in the amphibolite grade metamorphic pelites from the field area.



## 5. GEOTHERMOMETRY AND GEOBAROMETRY

### 5.1. Introduction

Reactions that involve pure phases have a single phase boundary on P-T diagrams. However reactions which involve solid solutions, in which the degree of solid solution exchange varies systematically with the P and T of crystallization, have a range of phase boundaries and the potential for being quantitative geothermometers and geobarometers. Examination of the composition of the co-existing mineral phases enables the estimation of P and T reached during metamorphism.

The best type of geothermometer is one with a near vertical phase boundary on the P-T diagram and which the temperature of crystallization is markedly affected by solid solution exchange.

A good geobarometer is one with a near horizontal phase boundary on the P-T diagram and with which the pressure of crystallization is markedly affected by solid solution exchange. (Wood & Fraser, 1977)

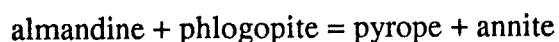
Several different methods have been applied to data from the study area. The data was obtained by microprobe analysis of available minerals in thin sections (appendix 3 , Table 3 ).

### 5.2 Geothermometry

A mineral assemblage occasionally found in the pelitic gneissic rocks of the study area that can be used for geothermometry are :

garnet- biotite- sillimanite- quartz- plagioclase.

Several thermometers have been suggested for garnet-biotite equilibria, each reliant on the determination of Fe-Mg partitioning between the two respective phases of the equation :



( see appendix 4 )

**5.2.1** Experiments on the equilibrium of synthetic mono-compositional garnets and variable biotites in the ratio 49:1, and in the temperature range 500-800°C,

conducted by Ferry and Spear (1978), enabled them to formulate a pressure-independent garnet-biotite geothermometer, for compositions close to ideal Fe-Mg binary compounds. The results obtained are averaged from six separate determinations, which were found to have a standard deviation of approximately  $\pm 20^{\circ}\text{C}$ . Using the Ferry and Spear equations the temperature range varies from  $580^{\circ}\text{C}$  at 4kb to  $610^{\circ}\text{C}$  at 12kb. (of 10)

Equations and detailed results in appendix 4.

**5.2.2** The more recent thermodynamic and statistical treatment of natural data with variable composition garnets allowed Ganguly and Saxena (1984) to suggest a modification of Ferry and Spears' (1978) experimental data on Fe-Mg fractionation between co-existing garnet and biotite. This data has been widely used for estimation of temperature of equilibration between natural garnet-biotite pairs, but mostly without proper regard for the compositional effects. Ganguly and Saxena's equations indicate temperature ranges from  $560^{\circ}\text{C}$  at 4kb to  $590^{\circ}\text{C}$  at 12kb. See Appendix 4 for equation substitutions and modifications.

**5.2.3** Indares and Martignole (1985) developed two models in an attempt to correct for solid solution impurities in P-T calculations. They allowed for compositional variations due to Ca and Mn substituting for Fe and Mg in garnet and Ti and Al(VI) substituting for Fe and Mg in biotite. The departure from ideality due to Ca in garnet can be calculated either with the available thermodynamic data (model A), or with a combination of thermodynamic and empirical data (model B), whereas that due to Mn is probably negligible due to the low Mn-content of high-grade garnets and biotites. For model A, the temperature ranges from  $540^{\circ}\text{C}$  at 4kb to  $570^{\circ}\text{C}$  at 12kb and for model B, the temperature ranges from  $630^{\circ}\text{C}$  at 4kb to  $660^{\circ}\text{C}$  at 12kb. what are  
equations  
about

The Mn content of the garnets ( 9.2- 9.75% ) and the high Ti content of the biotites ( 1.5- 1.6% ) from the study area is greater than the recommended amount and thus create inaccuracies in the results obtained. ( see Appendix 4 for parameters and equations ). The detailed results of these calculations can be seen in Table 4 (Appendix 4).



**5.2.3** An internally consistent data set has been developed by Powell and Holland (1985) in two parts. The first, consisting of applying a least squares approach to a simple system (i.e. Na<sub>2</sub>O-Al<sub>2</sub>O<sub>3</sub>-SiO<sub>2</sub>-H<sub>2</sub>O ), outlines the philosophy and methods of determining an internally consistent thermodynamic data set for minerals. In the second part, the model is applied to a much larger data set involving 60 reactions and 43 phases, in the system K<sub>2</sub>O-Na<sub>2</sub>O-CaO-MgO-Al<sub>2</sub>O<sub>3</sub>-SiO<sub>2</sub>-H<sub>2</sub>O-CO<sub>2</sub>, which solves the enthalpies of formation for the various reactions. Subsequent update to the data set includes <sup>Fe</sup>Ti-rich minerals ( Powell and Holland, 1988 )

They have used experimental data to obtain thermodynamic results for the reactions and are also able to calculate the errors involved in obtaining accurate pressures and temperatures.

This data is used in calculating the temperatures and pressures of rocks from the field area. A set of four reactions which are relevant to the sillimanite gneiss found in the field area are as follows:

- 1) 12sill + 3phl + 4gr = py + 12an + 3east
- 2) 18an + 3east = san + 15sill + 2phl + 6gr + H<sub>2</sub>O
- 3) 2q + sill + ann = san + alm + H<sub>2</sub>O
- 4) 3q + 2ann + 3an = 2an + 2alm + gr + H<sub>2</sub>O

Activity models are used to calculate the activity constants for each mineral present from the data obtained from microprobing, as follows;

Table (a) Activities

|    |         |        |         |         |         |
|----|---------|--------|---------|---------|---------|
|    | q       | san    | py      | alm     | sill    |
| a  | 1.00    | 1.00   | 0.0023  | 0.205   | 1.00    |
| sd | 0.0     | 0.0    | 0.67808 | 0.15156 | 0       |
|    | phl     | ann    | an      | gr      | east    |
| a  | 0.073   | 0.037  | 0.370   | +00002  | 0.045   |
| sd | 0.31958 | .40013 | 0.11907 | 1.10521 | 0.37244 |

Using the activity constants, the equilibrium constant (K) can be calculated and subsequently the pressures can be calculated. Table (b) shows the pressures calculated from the four reactions, with the temperature set at 650°C and using Gibbs free energy equation and Powell and Holland's data.

Pressures are also calculated for other set temperatures and the averages from the four equations are set out below.

| T C  | 600 | 625  | 650  | 675  | 700 |
|------|-----|------|------|------|-----|
| av P | ?   | 7.6  | 6.9  | 6.0  | ?   |
| sd   | -   | 2.36 | 2.09 | 2.04 | -   |
| f    | -   | 2.0  | 1.7  | 1.5  | -   |

The best estimates have the least error ; these being

6.9kb +/- 2.09 at 650°C and 6.0kb +/- 2.04 at 675°C

This analysis indicates that approximate temperatures and pressures that the gneissic rocks in the field area have undergone range from 4-8kbs at 650-675°C.

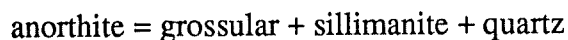
Table (b)

|        | P(T=650°C) | sd   | dP/dT   | lnK     |
|--------|------------|------|---------|---------|
| eqn.1. | 4.9        | 1.83 | 0.0135  | 23.822  |
| eqn.2. | 4.4        | 1.74 | 0.0087  | -42.953 |
| eqn.3. | 8.5        | 4.95 | -0.0653 | 1.712   |
| eqn.4. | 4.3        | 1.96 | -0.0091 | -4.413  |

*what about  
this*

### 5.3 Geobarometry

The only geobarometer applicable to the lithologies in the study area is that involving the reaction:



Application of this barometer to garnet-plagioclase assemblages allows other, more pressure dependent, P-T conditions to be calculated.

A model developed by Newton and Haselton (1981) from numerous experimental determinations of the univariant reaction has been made. Solid solution of  $\text{Ca}_3\text{Al}_2\text{Si}_3\text{O}_{12}$  with other components, principally almandine and pyrope, lowers the pressure at a given temperature at which the right hand assemblage is stable and solid solution of anorthite with albite in plagioclase tends to stabilize the left-hand side to higher pressures. The grossular component is usually quite dilute in natural garnets co-existing with plagioclase, an  $\text{Al}_2\text{SiO}_5$  polymorph and quartz so that the pressure lowering effect prevails. The pressure range obtained varies from 8.7kb at 500°C to 21.7kb at 1000°C ( see appendix 4 for equations and detailed results ).

This barometer also assumes Mn, Cr and Fe<sup>3+</sup> impurities in garnet are negligible. Experiments indicate that the impurity can be disregarded if Mn < Mg/3. This condition is not met (Garnet (Mn) value is higher in my samples), adding some increased uncertainty to the results.

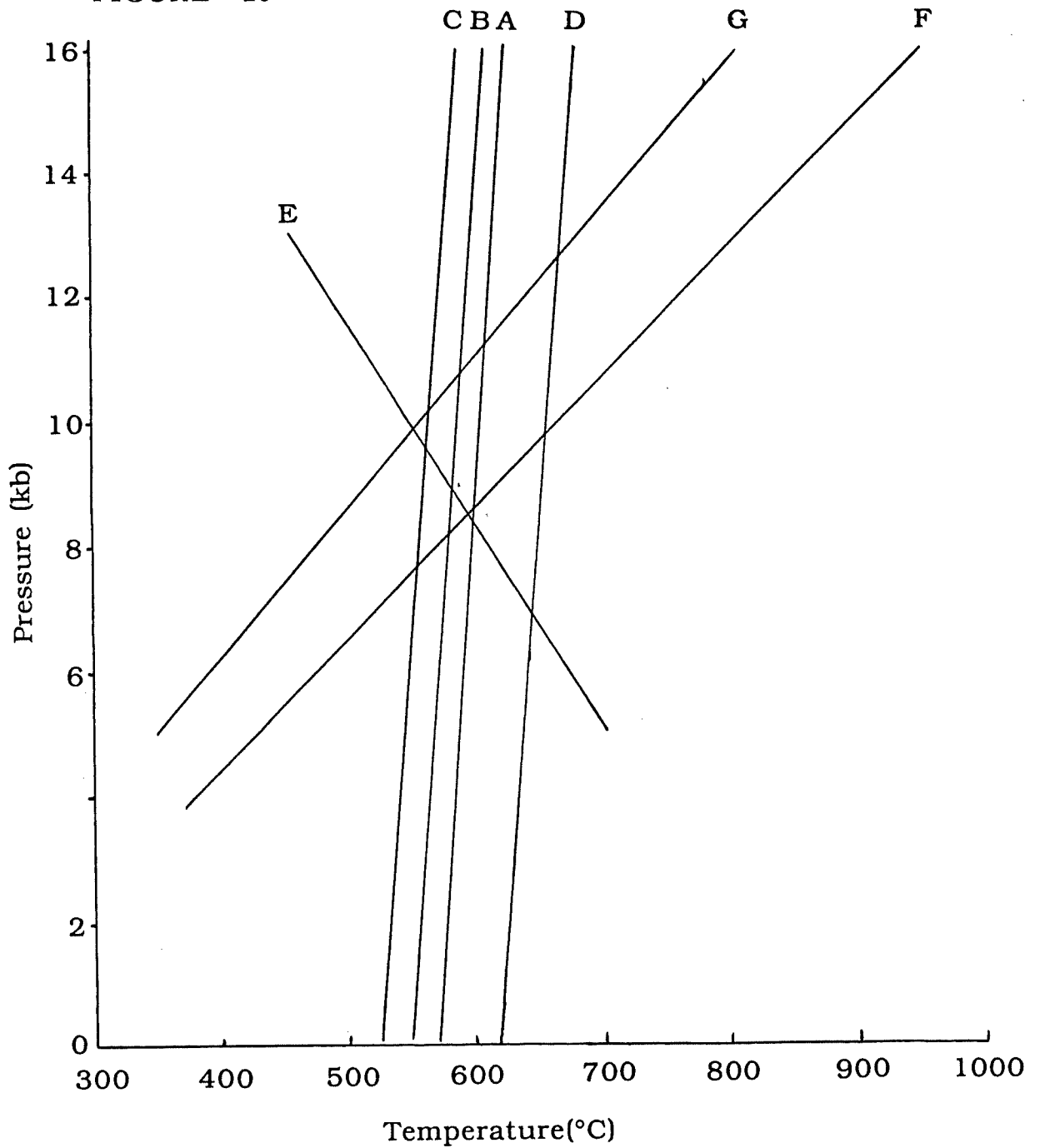
The An. model of Newton and Haselton above is based on empirical formulation; Saxena and Ribbie (1972) have derived an a An. model directly from thermodynamic and statistical analysis of experimental data. This gives lower pressures ranging from 6.5kb at 500°C to 17kb at 1000°C.

Taking all the above results in to account an average pressure and temperature can be estimated : approximately 8-10kb at 550-650°C.

These results are displayed graphically on a PT diagram (fig. 16) and values of probe analysis are listed in Table 3. (Appendix 3).

clearly  
very  
increased  
impurities  
pyrolytic  
stabilized

FIGURE 16



- A. Ferry and Spear (1978).
- B. Ganguly and Saxena (1984).
- C. Model A: Indares and Martingole (1985).
- D. Model B: Indares and Martingole (1985).
- E. Powell and Holland (1985).
  
- F. Saxena and Ribble (1972).
- G. Newton and Haselton (1981).

## **6. GEOCHRONOLOGY**

### **6.1. Purpose for dating**

For many years the Inlier rocks were assumed to be Archaean in age, as indicated on the Geological Survey Map of 1954. More recently, the estimate is Proterozoic in age, as found for the exposed basement to the north and west of South Australia.

By looking at the results obtained by earlier authors ( see chapter 1.2), there has been no conclusive evidence to indicate the age of the basement inlier rocks. Mineral ages, both U-Pb and Rb-Sr, have been grossly updated by the Delamerian Orogeny (see chapter 1.3). Some whole rock Rb-Sr measurements on the Houghton granulite ( 'diorite' ) have produced an isochron relationship interpreted as recording an upper amphibolite grade metamorphism at 860Ma ( Cooper & Compston, 1971). Obviously retrogressed samples are seen to be isotopically disturbed.

The basement rocks unconformably underlie rocks of the Proterozoic Adelaidean System. The basal unit of the Adelaidean, once thought to be as old as 1400Ma, has been demonstrated to be slightly older than 800Ma ( Fanning *et al.*, 1986 ). The U-Pb isotope method of dating zircon has been used to date a basement post-tectonic microgranite with the aim of placing a minimum age on the whole basement lithology and deformation. This method has proved useful in areas with later thermal disturbances such as the Delamerian event in this region.

### **6.2. Sampling and Dating Procedure**

Approximately 30kg of the fresh, unweathered microgranite(aplite) from the study area was collected for geochronological analysis. ( 896-11 on sample locality map in appendix 1 ). The aplite was chosen because it was found to intrude and cut across the gneissic rocks in the area and it was expected to contain a reasonable amount of zircons. It also looked relatively undeformed and unaltered. The rock was crushed and a zircon mineral concentrate extracted as outlined in appendix 5.

The colour of the zircons varied from clear crystals to darker pink-brown crystals. Most were clearly euhedral in shape, although some were fractured and others rounded. Some zircons which had to be removed were intergrown with a white, platy mineral. Other frosted zircons were air-abraded to remove the weathered edge.

As outlined in Appendix 5, six fractions of different size and magnetic properties were chosen to obtain a maximum spread on the concordia diagram, and consequently, an accurate as possible age.

Analytical procedures for the extraction of zircons from the aplite and sample preparation prior to analysis on the mass spectrometer are outlined in Appendix 5.

### 6.3 Results

The U-Pb isotopic data for the six fractions are plotted on the concordia diagram in figure 17 and details of U-Pb isotopic analyses can be found in Table 5 (Appendix 5).

The fractions are variably discordant with  $^{207}\text{Pb}/^{206}\text{Pb}$  ages ranging from 1538 Ma to 1570 Ma and the  $^{206}\text{Pb}/^{238}\text{U}$  ages ranging from 945 Ma to 1254 Ma. The relatively good spread of points produce a reasonably linear discordia on the  $^{207}\text{Pb}/^{235}\text{U}$  vs.  $^{207}\text{Pb}/^{235}\text{U}$  'concordia' diagram.

An appropriate regression (Ludwig, 1980) through the points produces an upper intercept of  $1578 \pm 22$  Ma, which would be interpreted as representing the age of crystallization of the aplite. The lower intercept of  $82 \pm 83$  Ma is much less concise and may indicate late stage tectonic uplifting that occurred in the Tertiary. The MSWD value of 10.4 indicates that the scatter from linearity is greater than expected experimental error. Some minor geological disturbance or presence of older inherited pre-magma zircon grains are the probable cause of this excess scatter. The overall effect of the Delamerian must be extremely small.

#### 6.4. Interpretation and Implications

By field observations it can be seen that the aplite intrusion post dates most, if not all, other rocks in the map area. This consequently sets a minimum age for the deposition of the rocks and also the deformation and metamorphic events the rocks have undergone.

The evidence of a Proterozoic age for a seemingly undeformed intrusive in the basement terrain suggests that the major deformational and metamorphic events described previously are all at least Proterozoic in age.

As the date of the lower intercept on the concordia diagram indicates the only isotopic disturbance to occur to the aplites' whole rock system has been sometime since the Late Cretaceous, this may be interpreted as the regional tectonic uplift that formed the present day ranges. The zircon mineral grains must have remained closed concordant systems until the cover removal following block faulting that occurred in the Tertiary.

As all previous authors have indicated, the basement inlier is the core of an anticline that was formed during the Delamerian Orogeny. The zircon chemical systematics were little affected by this gross disturbance.

Why  
is it better

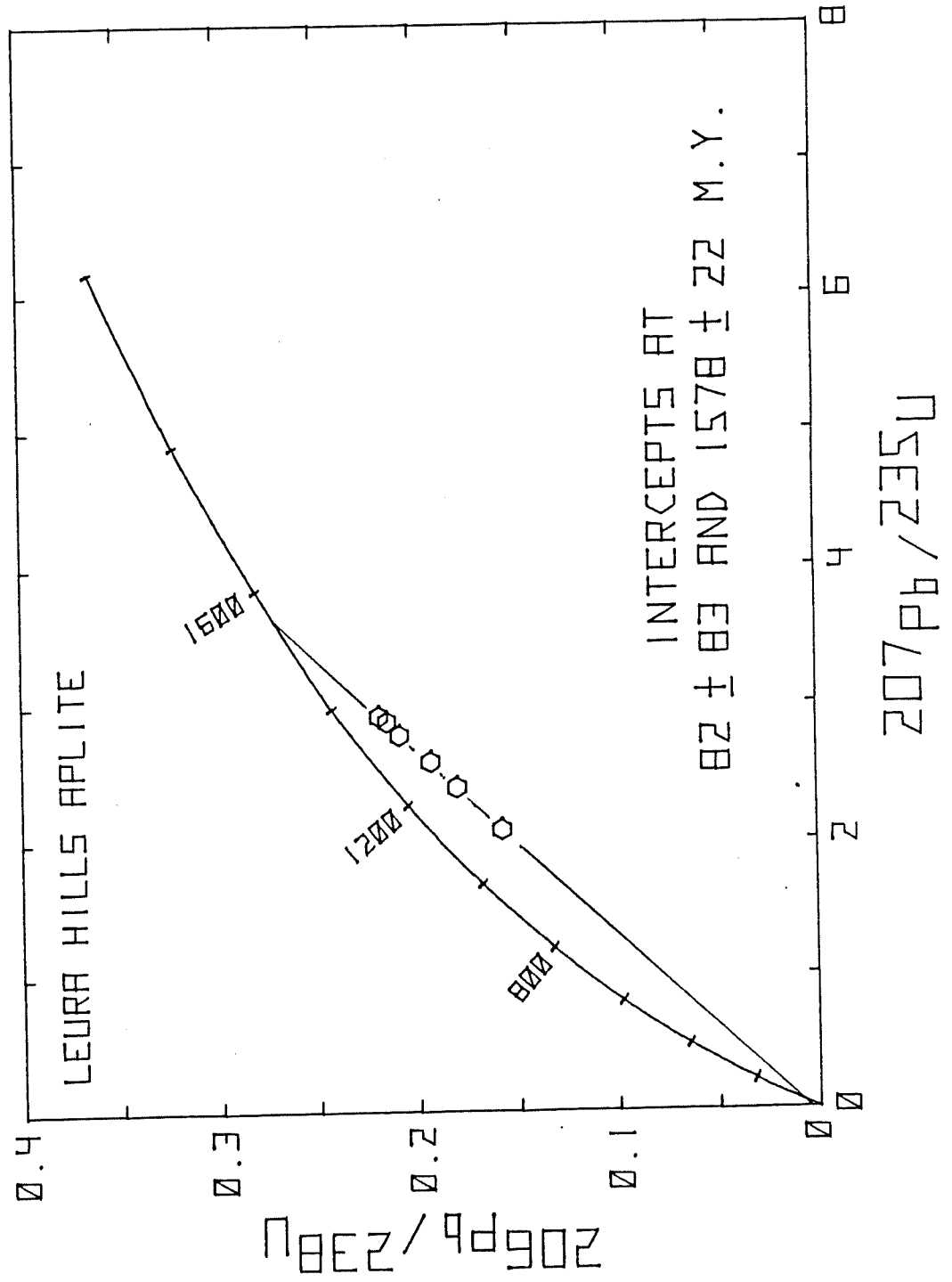


FIGURE 17 Concordia diagram showing data points of six zircon populations from the Leura Hills Aplitite.



## **7. CONCLUSIONS**

### **7.1. Comparison to other basement areas of S.A.**

On further investigation, it was found that the above date are similar to other dates obtained from post-tectonic intrusives on the Gawler Craton and the Olary Block (see fig. 1 ). The Charleston Granite from the Hutchinson Group of metamorphic and intrusive rocks near Cowell on the Eyre Peninsula ( Parkin, 1969), has a closely comparable age to the aplite in my study area, as is a granite body near Crocker Well in the Olary Block, in the North East of S.A. which is a part of the metamorphic and intrusive Willyama Complex ( Rutland, 1981).

The rocks of each area are not only comparable in age, but also in their compositions, metamorphics and structural history, which are outlined in Table 6.

This interpretation leads to at least one conclusion: widely separated blocks of South Australian Proterozoic basement rocks have many similarities in their geological history. This indicates an originally large homogeneous terrain during the Early Proterozoic, which subsequent tectonic events have altered, and of which only isolated areas still remain exposed.

TABLE 6.

Myponga-Yankalilla Inlier, S. A.

Dates of comparable igneous intrusions.

Microgranite- 1578-\+22Ma.

Structure and Metamorphism

The inlier rocks have undergone a complex history of deformation and metamorphism. An original metamorphic event of upper amphibolite grade produced S1 gneissic layering (no recognized F1). F2 folding has been recognized in the gneisses as tight to isoclinal folding and S2 fabric, nearly parallel to S1.

A third deformation period produced an S3 schistosity which cuts S2 and larger more open F3 folding.

The final deformation produced a distinct, near vertical schistosity (S4) that is prominent in the retrograde greenschist metamorphosed schists.

Basic dykes and a phase of pegmatite intrusion occurred pre-D2.

A phase of late-tectonic intrusions (pegmatite and aplite) occurred during or after the final deformation.

Olary Province, S. A.

Date of comparable igneous intrusion.

Crocker Well granite- 1579+\-2Ma (Ludwig & Cooper, 1984)

Structure and Metamorphism

The Olary province is the western part of the Willyama Block, a promontory of the Gawler province of the Precambrian shield of Australia.

The summary by Rutland (1981), suggests that the Willyama Complex was a sequence of shallow-water deposits which experience three early deformational events. Each of these was accompanied by metamorphism, the first being high grade (amphibolite).

The third metamorphic event was lower grade and was accompanied by the intrusion of late tectonic granitoids and pegmatites, all occurring during the Proterozoic.

Later Delamerian metamorphism, deformation and intrusions are also evident in the area.

Gawler Craton, S. A.

Charleston Granite-1590Ma (Parkin, 1969.)

Structure of Cleve sub-domain- (Lemon & Parker, 1982)

It is a major Early to Middle Proterozoic orogenic belt or 'mobile zone'. It can be divided into two parallel zones. The western zone is characterised by a sequence of highly metamorphic and deformed sediments, including quartzites, schists and gneisses, dolomites, iron formations and amphibolites, collectively known as the Hutchinson Group.

These are tightly interfolded with a variety of older granitic gneisses and all are intruded by various synorogenic granites.

By contrast the eastern zone is characterised by a sequence of less intensely deformed and metamorphosed acid volcanics, hornblende gneisses, schists and amphibolites, with only late or post-orogenic intrusions evident. Kimbrian Orogeny (1820-1580Ma)- regional amphibolite grade metamorphism and schistosity (D1), overturned isoclinal folding (D2) and upright open folding and mylonisation (D3). Later folding occurred during the Warfakian Event (1500-1450Ma).

## ACKNOWLEDGEMENTS

I wish to thank Dr John Cooper for organizing and supervising my project throughout the year.

Many thanks to Drs. Mike Sandiford and Robin Oliver for helpful discussion and advice.

I am grateful to the technical staff of the Geology Department for their invaluable help this year. Especially to David Bruce, whose help with the geochronological techniques and the running of the mass spectrometer is much appreciated; Geoff Trevellyan and Wayne Mussared for thin sectioning; Evert Bleys and Rick Barrett for photography; Phil McDuire and John Stanley for whole rock analyses; John Willoughby for computing; Sherry Proferes for drafting and Nick Lemon and Sally Phillips for eleventh hour contributions' and also Hew for help with probe..

Many thanks go to my fellow honours colleagues and my friends, especially Bob, who have made the year quite enjoyable

Deepest appreciation goes to my family for their support and encouragement throughout my years at University and especially my thanks go to Noelene for unfailing support, patience and understanding.

## REFERENCES

- Alderman, A.R. (1938). Augen gneisses in the Humbug scrub area, South Australia. Trans.R.Soc.S.Aust., 62; 168-181.
- Benson, W.N. (1909a). Petrological notes on certain Precambrian rocks of the Mount Lofty Ranges, with special reference to the geology of the Houghton District. Trans.Roy.Soc.S.Aust., 33; 226-241.
- Campana, B. (1954). Absolute age of uraniferous granite and Precambrian tillite in the Crockers Well area. ( Olary District ) Aust.J.Sci., 16; 240-241.
- Campana, B. (1955b). The structure of the eastern S.A. ranges: The Mt.Lofty Arc. J.Geol.Soc.Aust., 2; 47-61.
- Cooper, J.A. and Compston, W. (1971). Rb-Sr dating within the Houghton Inlier, S.A. J.Geol.Soc.Aust., 17; 213-219.
- Davies, M.D. (1972). A. The geology and petrology of an Archean Inlier south of Normanville. B. The geochemistry of the 'Houghton' granulite. University of Adelaide Hons. thesis, unpubl.
- England, H.N. (1935). Petrographic notes on intrusions of the Houghton Magma in the Mt.Lofty Ranges. Trans.Roy.Soc.S.Aust., 59; 1-15.
- Ehlers, E.G. and Blatt, H. (1980). Petrology: Igneous, Sedimentary and Metamorphic. (W.H. Freeman & Company, San Francisco).

- Fanning, C.M. (1984). Rb-Sr dating of three samples from Torrens Gorge, near Prairie. Amdel Report GS6473-84. S.Aust.Dept. Mines & Energy open file ENV 6713 (unpubl.)
- Fanning, C.M., Ludwig, K.R., Forbes, B.G. and Priess, W.V. (1986). Single and multiple grain U-Pb zircon analysis for the Early Adelaidean Rook Tuff, Willouran Ranges, S.A. IN: 8th Australian Geological Convention, 1986, Abstr.Geol.Soc.Aust., 15; 71-72.
- Ferry, J.M. and Spear, F.S. (1978). Experimental calibration of the partitioning of Fe & Mg between biotite and garnet. Contrib.Min.Pet., 66; 113-117.
- Forbes, B.G. (compiler) (1979). Onkaparinga map sheet, Geological Atlas of S.A., 1:50,000 series. sheet 6628-11. Geol.Surv.S.Aust.
- Ganguly, J. and Saxena, S.K. (1984). Mixing properties of aluminosilicate garnets: constraints from natural and experimental data, applications to geothermo-barometry. American Mineralogist, 69; 88-97.
- Glaessner, M.F. and Parkin, L.W. (eds.) (1958). The geology of S.A. - prepared by members of the S.A. division of the Geol.Soc.Aust. (Melb. Uni. Press, Melbourne).
- Greenhalgh, D. and Jeffery, P.M. (1959). A contribution to the Precambrian geology of Australia. Geochem. Cosmochim. Acta, 16; 39-47.

- Holm, P.E. (1985). The geochemical fingerprints of different tectonomagmatic environments using hygromagmatophile element abundances of tholeiitic basalts and basaltic andesites. Chemical Geology, 51; 303-323.
- Hossfeld, P.S. (1935). The geology of part of the North Mt. Lofty Ranges. Trans. Roy. Soc. S. Aust., 59; 16-67.
- Howchin, W. (1906). The geology of the Mt. Lofty Ranges. Part II. The lower and basal beds of the Cambrian. Trans. Roy. Soc. S. Aust., 30; 227-262.
- Hubbard, E.W. (1965). Antiperthite and Mantled feldspar textures in Charnockite (enderbite) from Southwest Nigeria. American Mineralogist, 50; 2040-2051.
- Indares, A. and Martignole, J. (1985). Biotite-garnet geothermometry in the granulite facies: the influence of Ti and Al in biotite. American Mineralogist, 70; 272-278.
- Kleeman, A.W. (1946). An age determination on samarskite from Mt. Painter, S.A. Trans. Roy. Soc. S. Aust., 70; 175-177.
- Lemon, N.M. and Parker, A.J. (1982). Reconstruction of the Early Proterozoic stratigraphy of the Gawler Craton, S.A. J. Geol. Soc. Aust., 29; 221-238.
- Ludwig, K.R. (1980). Calculation of uncertainties of U-Pb isotope data. Earth. Planet. Sci. Lett., 46; 212-220.

- Ludwig, K.R. and Cooper, J.A. (1984). Geochronology of the Precambrian granites and associated U-Ti-Th mineralization, northern Olary Province, S.A. Contrib.Min.Pet. (Springer-Verlag, Amsterdam.)
- McEwin, A.J. (1972). Geology and petrology of part of the Archaean Inlier, northeast of Yankalilla, Fleurieu Peninsula. Hons. Thesis (unpubl.)
- Meschede, M. (1986). A method of discriminating between different types of mid-ocean ridge basalts and continental tholeiites with the Nb-Zr-Y diagram. Chemical Geology, 56; 207-218.
- Mullen, E.D. (1983). MnO-TiO<sub>2</sub>-P<sub>2</sub>O<sub>5</sub> ; a minor element discrimination for basaltic rocks of oceanic environments and its implication for petrogenesis. Earth.Planet.sci.Lett., 62; 53-62.
- Newton, R.C. and Haselton, H.T. (1981). Thermodynamics of the garnet-plagioclase-Al<sub>2</sub>SiO<sub>5</sub>-quartz geobarometer. IN; Newton, R.C., Natrotsky, A. and Wood, B.J. (eds) Thermodynamics of minerals and melts. (Springer, New York), pp 129-138.
- Offler, R. and Fleming, P.D. (1968). A synthesis of folding and metamorphism in the Mt.Lofty Ranges, S.A. J.Geol.Soc.Aust., 15 (2); 245-266.
- Parkin, L.W. (editor) (1969). Handbook of 'South Australian Geology. (Geological Survey of South Australia, Adelaide).

- Pearce, J.A. and Cann, J.R. (1973). Tectonic setting of basic volcanic rocks determined using trace element analysis. Earth.Planet.Sci.Lett., 19; 290-300.
- Pearce, J.A. (1975). Basalt geochemistry used to investigate post tectonic environment on Cyprus. Tectonophysics, 25; 41-68.
- Pearce, T.H., Gorman, B.E. and Birkett, T.C. (1975). The TiO<sub>2</sub>-K<sub>2</sub>O-P<sub>2</sub>O<sub>5</sub> diagram: A method of discriminating between oceanic and non-oceanic basalts. Earth.Planet.Sci.Lett., 24; 419-426.
- Pettijohn, F.J. (1957). Sedimentary Rocks. (Harper and Row, New York).
- Powell, R. and Holland, T.J.B. (1985). An internally consistent thermodynamic dataset with uncertainties and correlations: 1. Methods and a worked example. J.Metamorphic.Geol., 3; 327-342.
- Powell, R. and Holland, T.J.B. (1985). an internally consistent thermodynamic dataset with uncertainties and correlations: 2. Data and results. J.Metamorphic.Geol., 3; 343-370.
- Powell, R. and Holland, T.J.B. (1988). An internally consistent thermodynamic dataset with uncertainties and correlations: 3 J.Metamorphic Geology, 3; 327-342.
- Radke, F. and Webb, A.W. (1975). Geochronology of the eastern basement rocks- Amdel progress report no.7 S.Aust.Dept. Mines and Energy open file ENV. 2136 (unpubl.).

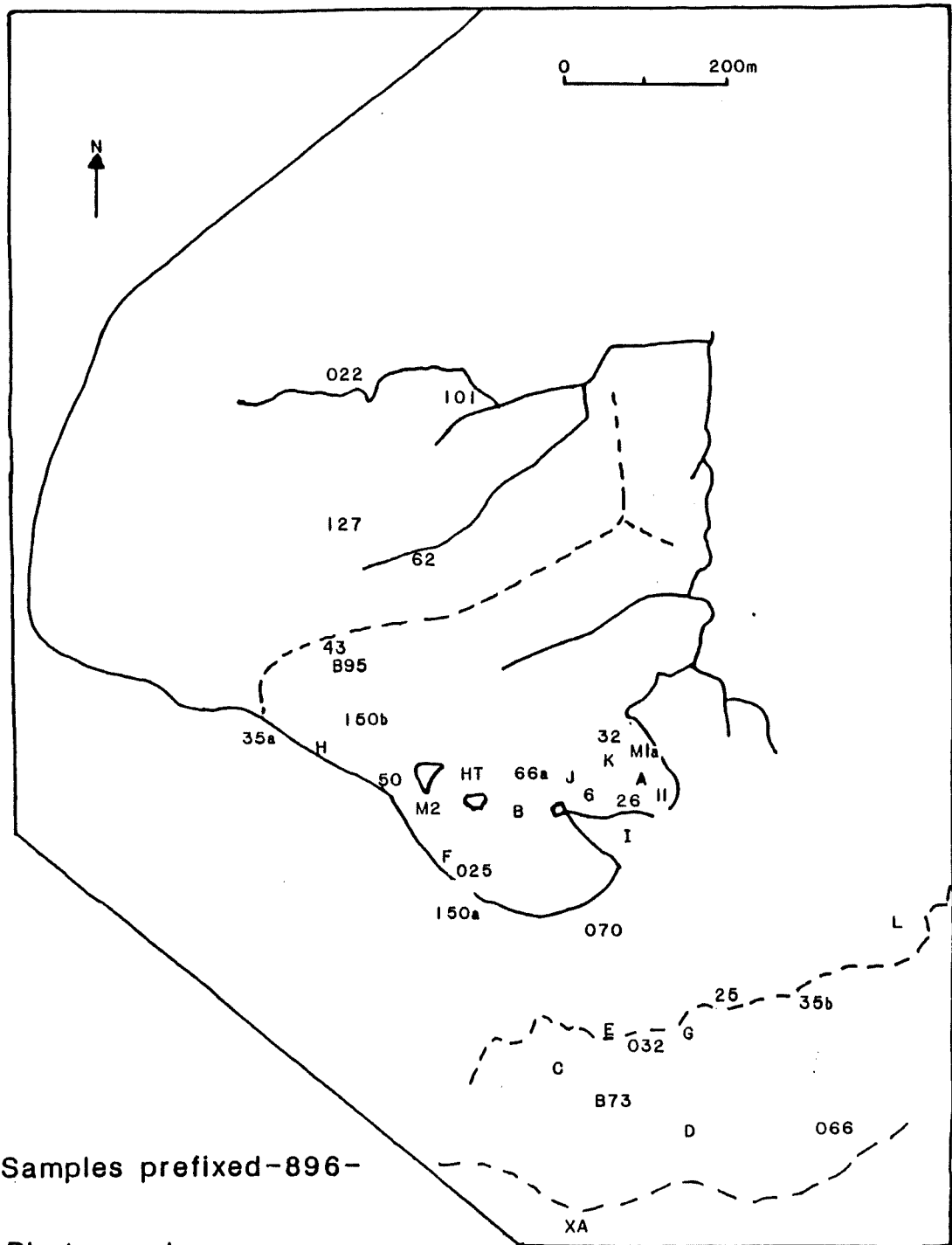


- Rutland, R.W.R. (1981). Structural framework of the Australian Precambrian. In, Hunter, D.R. (ed) Precambrian of the Southern Hemisphere. (Elsevier, Amsterdam). pp 1-37.
- Saxena, S.K. and Ribbie, P.H. (1972). Activity- composition relations in feldspars. Contrib.Min.Pet., 37; 131-138.
- Shervais, J.W. (1982). Ti-V plots and the petrogenesis of modern and ophiolitic lavas. Earth and Planet.Sci.Lett., 59; 101-108.
- Spry, A.H. (1951). The Archaean Complex at Houghton, S.A. Trans.Roy.Soc.S.Aust., 74; 115-134.
- Talbot, J.L. (1963). Retrograde metamorphism of the Houghton Complex, S.A. Trans.Roy.Soc.S.Aust., 87; 185-196.
- Thomas, R.G. (1924). A monazite-bearing pegmatite near Normanville. Trans.Roy.Soc.S.Aust., 48; 256-268.
- Thomson, B.P. and Horwitz, R.C. (1962). Barker 1:250,000 Map Sheet, Geological Survey of S.A. (Dept.Mines., Adelaide).
- Winchester, J.A. and Floyd, P.A. (1977). Geochemical discrimination of different magma series and their differentiation products using immobile trace elements. Chem.Geol., 20; 325-345.
- Wicks, S.P. (1972). Geology of part of the basement inlier north-east of Mt. Compass. University of Adelaide Hons. thesis, unpubl.
- Winkler, H.G.F. (1965). Petrogenesis of metamorphic rocks. (Springer Verlag, Amsterdam).

Wood, B.J. and Fraser, D.G. (1977). Elementary thermodynamics for geologists. (Oxford University press, Oxford).


APPENDIX 1  
SAMPLE LOCALITY AND OBSERVATION MAP,  
MODAL ANALYSIS, HAND SPECIMEN AND  
THIN SECTION DESCRIPTION.

# Sample and Observation Locality Map



Samples prefixed-896-

Photographs: a-m

vehicle track 

creeks 

In this appendix, approximate modal analyses, as well as representative hand specimens and thin section descriptions are given for each of the lithologies studied.

| Quartz-biotite gneiss |     |     |       |     |
|-----------------------|-----|-----|-------|-----|
| 896-                  | 6   | 66a | M2    | 032 |
| Quartz                | ~45 | ~50 | 15    | ~45 |
| Plagioclase           | 5   | -   | ~35   | 30  |
| K-feldspar            | 5   | ~5  | ~5    | 15  |
| Sericite              | 35  | 35  | 5     | -   |
| Biotite               | 10  | 10  | 40    | 10  |
| opaques               | ~2  | 2   | trace | ~2  |

#### Sample 896-6

Hand specimen : Light coloured coarse grained rock. It shows a strong lineation and the rock is dominated by quartz, feldspar and minor biotite.

Thin section : The section was cut across the lineation and shows mostly equant crystals of quartz ( 0.2-0.5mm ), which do not show any signs of deformation features. They are clear under plain polarised light (UPL) and grey to black under crossed polars (UXP). Most of the feldspar has been entirely altered to a fine grain mosaic of sericite, but there is still some plagioclase and microcline left. Sericite appears as corroded grey crystals (UPL) and multiple colours, from grey to high blues (UXP).

The biotite appears as elongate crystals and show dark brown to fawn coloured pleocroism (UPL). Some red staining and corroded edges indicate alteration. The biotites show high birefringent colours up to bright greens and parallel extinction ( 0.2-0.5mm ).

A minor percentage (1-2%) of very dark coloured opaques appear, which have a reasonable sub-anhedral shape.

Sillimanite gneiss

| 896-        | 26    | 32  | M1a   |
|-------------|-------|-----|-------|
| Quartz      | ~40   | ~65 | ~55   |
| Plagioclase | trace | -   | -     |
| K-feldspar  | 5     | -   | -     |
| Sericite    | 30    | 20  | 30    |
| Biotite     | 15    | ~10 | 10    |
| Sillimanite | 10    | ~5  | ~5    |
| Garnet      | trace | -   | ~2    |
| opaque      | ~2    | ~2  | trace |

Sample 896-26

Hand specimen : Light coloured coarse grained rock. It shows a strong lineation of the major constituents; quartz, biotite and sillimanite.

Thin section : The quartz crystals look the same as the previous sample, except they are bigger ( 0.5-1mm ). Once again the feldspars are nearly completely altered to sericite, which appears as a fine grained mosaic of mottled grey crystals (UPL) and show multiple high birefringent colours (UXP). The plagioclase does show twinning and there are small amounts of perthite to be seen.

The biotite is very similar to above sample. Sillimanite appears as well shaped crystals with high relief. The section was cut at right angles to their length. The crystals are diamond shaped with a strong cleavage that cuts the crystals diagonally. They show low birefringent colours in this orientation. In the samples cut length wise the crystals are elongate and fiborous in nature and show higher birefringent colours.

The garnets are small and broken up. They have no distinct shape and appear to be rimmed or altered. They show high relief and are isotropic (UXP).

The opaques appear as black, sub-hedral shaped minerals (haematite or magnetite. )

Quartzo-feldspathic gneiss

| 896         | 101 | 066 | 43    |
|-------------|-----|-----|-------|
| Quartz      | 10  | 10  | 40    |
| Plagioclase | 30  | 30  | 10    |
| K-feldspar  | 5   | -   | -     |
| Perthite    | 20  | 10  | 10    |
| Sericite    | -   | -   | 30    |
| Hornblende? | 30  | ~20 | -     |
| Diopside?   | -   | ~20 | -     |
| epidote     | -   | -   | 10    |
| opaque      | 5   | 10  | trace |

Sample 896-101

Hand specimen : Light coloured, equigranular, reasonably crystalline medium grained rock. Observable minerals are quartz, feldspar and ?diopside. There is a faint segregation layering.

Thin section : Quartz is similar to above sample. The feldspars show regrowth and intergrowth of crystals; from intergrown microcline crystals to large single crystals of plagioclase (1-2mm). A texture developed during high-grade metamorphism, rather than during crystallization of magma. Probe analysis indicated that some randomly orientated inclusions in the plagioclase are K-feldspar.

The hornblende appear as light brown to light green, slightly pleochroic crystals. They show good cleavage and medium to high colours (UXP). They are corroded at the edges and along the cleavages. Probe analysis indicates the opaque inclusions that appear in the hornblende are ilmenite. Also probe analysis suggests that the amphibole formed from the breakdown of the pyroxene; diopside.

Sample 896-43

Hand specimen : The rock is quite weathered and crumbles easily. It is a medium to coarse grained rock and shows some semblance of preferential quartz-rich layers. It is a white rock consisting predominantly of quartz and feldspar, with minor quantities of dark minerals.

Thin section : Quartz appear as large crystals (1-2mm) and show preferred layering and undulose extinction. The feldspars are mainly plagioclase, which has been badly sericitized, but still shows obvious twinning. There are a few perthitic textures to be seen, also.

Epidote appears as small crystals (< 0.5mm), with random orientation and are usually found as inclusions in the feldspar. They are pleochroic, fawn to tan-yellow in colour and show high colours (UXP). Opaques appear randomly as inclusions in the other crystals.

#### Quartz-biotite Schist

| 896        | 022 | XA | 62 |
|------------|-----|----|----|
| quartz     | 65  | 80 | 60 |
| biotite    | 10  | 5  | 5  |
| muscovite  | 10  | 15 | 35 |
| feldspar   | 5   | -  | -  |
| actinolite | 10  | -  | -  |

Sample 896-022

Hand specimen : Shows strong directional properties with quartz-feldspar rich layers which are equigranular and medium grained. There are randomly orientated dark minerals with in this layer. They are divided by thin dark, mica rich layers. At another angle it can be seen that the elongate micas show a very strong preferred orientation. Two shearing directions can be seen showing this effect.



Thin section : They are dominated by large, reasonably equigranular crystals that have dusty inclusions. Feldspar is quite altered and rarely sighted. All the micas are stretched out to a point that they look fibrous. Muscovite appears as clear, elongate crystals that show high colours (UXP). Actinolite appears as elongate crystals with good cleavage. They show green to fawn pleochroism and low colours (UXP). The biotite appears as described before, except that it is more elongate.

Amphibolite

|             |    |
|-------------|----|
| 896-        | 50 |
| plagioclase | 30 |
| amphibole   | 65 |
| opaques     | 10 |
| muscovite   | 5  |

Sample 896-50

Hand specimen : A very dark, fine grained, massive rock which shows no layering or obvious deformation. Equigranular crystals of feldspar and dark minerals can be seen.

Thin section : Feldspar appears as randomly orientated, interlocking crystals showing twinning. Probe analysis shows them to be labrodorite; of the plagioclase series.

The amphiboles appear as anhedral, corroded crystals which are pale to dark green in colour. (UXP) they show very mottled low birefringent colours. Probe analysis indicate them to be of the actinolite-tremolite series.

The very dark, randomly distributed opaques are ilmenite.

Pegmatite

|             |       |       |    |
|-------------|-------|-------|----|
| 896-        | 35    | 025   | 25 |
| quartz      | 60    | 10    | 10 |
| plagioclase | 5     | 50    | 10 |
| K-feldspar  | -     | 5     | 15 |
| perthite    | 30    | 25    | 45 |
| biotite     | 5     | trace | 15 |
| opaques     | trace | 10    | -  |

Sample 896-25

Hand specimen : It appears as a crystalline, equigranular rock that is very coarse grained. Large crystals of quartz, feldspar and biotite can be seen.

Thin section : Quartz crystals are clear and large ( 0.5- 1mm). The feldspars appear as white mottled crystals. The perthite shows differing angles of extinction, where the intergrown lamellae of plagioclase show near parallel extinction, whereas the K-feldspar has an extinction angle 10 to 15 degrees off the parallel.

Biotite appears as creamy coloured to light brown pleochroic crystals and show high birefringent colours (UXP). Some show alteration features around the edges and along the cleavages.

Aplite/Microgranite

|            |       |       |
|------------|-------|-------|
| 896-       | 11    | 070   |
| quartz     | 30    | 30    |
| perthite   | 65    | 65    |
| biotite    | ~2    | ~2    |
| hornblende | 2     | trace |
| muscovite  | trace | -     |

Sample 896-11

Hand specimen : Appears as a light-pink coloured, dominantly feldspar and quartz rich rock, with minor amounts of biotite. The crystals are equigranular and medium to coarse grained. It is a very hard, crystalline rock that shows no obvious deformation or metamorphic features.

896-11 feldspar luster & sericitized along cracks & inter grain spaces  
 Quartz slight undulose extinction  
 Biotite ragged but unaltered  
 intergrown Qtz & felds  
 No directionalizing of elongated grains.

Thin section : Quartz appears (as before.) Feldspar is mostly perthite and shows exsolution features, with mostly plagioclase lamellae found in the K-feldspar crystals. Crystals are large and uncorroded ( 1-2mm ).

The biotite appears as elongate, cleavaged crystals, which are corroded at the edges. They show creamy-fawn to dark-brown pleochroism and bright colours (UXP).

A minor amount of hornblende appear as dark brown, non-pleochroic, anhedral shaped crystals, with a subtle cleavage.

APPENDIX 2

GEOCHEMICAL ANALYSIS : a) METHOD OF WHOLE ROCK ANALYSIS,  
AND b) MAJOR AND TRACE ELEMENT ANALYSIS AND  
NORMATIVE COMPOSITIONS

## APPENDIX 2 : ANALYTICAL METHODS.

Sample preparation for whole rock analysis.

(1) A core of fresh unweathered sample was obtained by trimming the edges off the rock.

(2) The sample was crushed in the jawcrusher and pulverised in the Siebtechnik tungsten carbide mill, to a very fine powder.

(3) An accurate amount of sample was placed in a platinum crucible, and ignited to 960C for 16 hours, to drive off volatiles. The loss on ignition (LOI) was calculated.

(4) Fused discs were prepared by fusing a mixture of the following components :

- (a) 0.02 gm of  $\text{NaNO}_3$ .

- (b) 0.28 gm of ignited sample.

- (c) 1.50 gm of flux.

(5) Major element oxides were analysed with the Siemens XRF using the fused discs.

(6) Using a pressing vessel and a hydraulic press, pressed pellets were made, using a boric acid powder backing. Trace element concentrations were determined using X-ray fluorescence spectrometry.

(7) Sodium concentration analyses were determined by digesting an accurate amount of sample (50-60gm) in a teflon beaker containing hydrofluoric acid (10ml), 50% sulphuric acid and water (10-20ml). The mixture was heated for 16 hours at approximately 125C and the resultant solution diluted to 100ml with distilled water in a volumetric flask and stored in a plastic bottle to prevent leaching of silica from glass. The sodium concentration of the solution was determined using atomic absorption spectrometry, and results were converted to % $\text{Na}_2\text{O}$ .

WHOLE ROCK ANALYSIS

PREFIXED  
896-

APLITE

| SAMPLE #                       | . 11a | .11b  | .11c  |
|--------------------------------|-------|-------|-------|
| <b>Major element (Wt%).</b>    |       |       |       |
| SiO <sub>2</sub>               | 73.6  | 80.39 | 73.75 |
| Al <sub>2</sub> O <sub>3</sub> | 14.39 | 11.06 | 14.28 |
| Fe <sub>2</sub> O <sub>3</sub> | 0.43  | 0.13  | 0.45  |
| MnO                            | 0     | 0     | 0.01  |
| MgO                            | 0.31  | 0.13  | 0.26  |
| CaO                            | 0.54  | 0.8   | 0.61  |
| Na <sub>2</sub> O              | 3.93  | 3.69  | 3.98  |
| K <sub>2</sub> O               | 5.58  | 2.67  | 5.36  |
| TiO <sub>2</sub>               | 0.13  | 0.19  | 0.12  |
| P <sub>2</sub> O <sub>5</sub>  | 0.13  | 0.04  | 0.1   |
| H <sub>2</sub> O-              | 0.36  | 0.27  | 0.35  |
| TOTAL                          | 99.4  | 99.38 | 99.27 |
| <b>Trace elements (ppm).</b>   |       |       |       |
| Sr                             | 74    | 85    | 84    |
| Rb                             | 162   | 57    | 148   |
| Y                              | 213   | 9.3   | 133   |
| Ba                             | 575   | 442   | 556   |
| Sc                             | 5.7   | 1.9   | 5.5   |
| Ni                             | 2     | 3     | 3     |
| V                              | 9     | 3     | 8     |
| Cr                             | 5     | 5     | 5     |
| Ga                             | 20    | 16    | 21    |
| Ce                             | 96    | 34    | 88    |
| Nd                             | 59    | 12    | 47    |
| La                             | 95    | 18    | 76    |
| Zr                             | 35    | 63    | 54    |
| Nb                             | 18.1  | 25    | 24    |
| <b>CIPW Norms.</b>             |       |       |       |
| Ap                             | 0.28  | 0.25  | 0.22  |
| Il                             | 0.25  | 0.24  | 0.23  |
| Mt                             | 0.24  | 0.23  | 0.25  |
| Or                             | 32.68 | 32.05 | 31.43 |
| Ab                             | 32.96 | 33.29 | 33.43 |
| An                             | 1.81  | 2.15  | 2.36  |
| Di                             |       |       |       |
| Hy                             | 0.56  | 0.53  | 0.5   |
| Ol                             |       |       |       |
| Ac                             |       |       |       |
| C                              | 2.41  | 2.26  | 2.11  |
| Q                              | 27.85 | 28.15 | 28.4  |

PEGMATITE

| SAMPLE # -35a -35b   |       |       |
|----------------------|-------|-------|
| Major element (Wt%)> |       |       |
| SiO2                 | 65.65 | 65.69 |
| Al2O3                | 14.38 | 14.61 |
| Fe2O3                | 6.29  | 5.92  |
| MnO                  | 0.03  | 0.03  |
| MgO                  | 2.21  | 2.22  |
| CaO                  | 0.75  | 0.76  |
| Na2O                 | 3.98  | 3.81  |
| K2O                  | 4.85  | 4.87  |
| TiO2                 | 0.86  | 0.78  |
| P2O5                 | 0.13  | 0.13  |
| H2O-                 | 0.4   | 0.44  |
| TOTAL                | 99.54 | 99.26 |
| Trace element (ppm). |       |       |
| Sr                   | 92    | 91    |
| Rb                   | 208   | 197   |
| Y                    | 15    | 17.2  |
| Ba                   | 433   | 416   |
| Sc                   | 13.8  | 13.1  |
| Ni                   | 33    | 33    |
| V                    | 64    | 66    |
| Cr                   | 67    | 67    |
| Ga                   | 21    | 19    |
| Ce                   | 150   | 134   |
| Nd                   | 67    | 58    |
| La                   | 88    | 85    |
| Zr                   | 196   | 210   |
| Nb                   | 15.1  | 15.2  |
| CIPW Norms.          |       |       |
| Ap                   | 0.3   | 0.29  |
| Il                   | 1.69  | 1.52  |
| Mt                   | 3.61  | 3.39  |
| Or                   | 32.74 | 29.4  |
| Ab                   | 34.82 | 32.94 |
| An                   | 2.97  | 2.99  |
| Di                   |       |       |
| Hy                   | 5.32  | 5.22  |
| Cl                   |       |       |
| Ac                   |       |       |
| C                    | 2.03  | 4.09  |
| Q                    | 16.16 | 18.98 |

AMPHIBOLITE

| SAMPLE #                       | 150a   | 150b  | B73    |
|--------------------------------|--------|-------|--------|
| <b>Major element (Wt%).</b>    |        |       |        |
| SiO <sub>2</sub>               | 50.54  | 50.37 | 50.42  |
| Al <sub>2</sub> O <sub>3</sub> | 13.08  | 13.08 | 13.28  |
| Fe <sub>2</sub> O <sub>3</sub> | 15.63  | 15.5  | 15.6   |
| MnO                            | 0.25   | 0.24  | 0.23   |
| MgO                            | 5.99   | 5.51  | 5.89   |
| CaO                            | 9.71   | 9.68  | 9.79   |
| Na <sub>2</sub> O              | 2.23   | 2.21  | 2.24   |
| K <sub>2</sub> O               | 0.48   | 0.47  | 0.54   |
| TiO <sub>2</sub>               | 1.74   | 1.7   | 1.73   |
| P <sub>2</sub> O <sub>5</sub>  | 0.19   | 0.19  | 0.18   |
| H <sub>2</sub> O-              | 0.38   | 0.37  | 0.35   |
| TOTAL                          | 100.23 | 99.35 | 100.27 |
| <b>Trace elements.</b>         |        |       |        |
| Sr                             | 157    | 151   | 148    |
| Rb                             | 19.7   | 19.9  | 30     |
| Y                              | 42     | 42    | 38     |
| Ba                             | 388    | 233   | 138    |
| Sc                             | 4      | 44    | 44     |
| Ni                             | 49     | 49    | 44     |
| V                              | 392    | 395   | 392    |
| Cr                             | 51     | 58    | 56     |
| Ga                             | 22     | 19    | 20     |
| Ce                             | 37     | 40    | 30     |
| Nd                             | 25     | 22    | 20     |
| La                             | 19     | 20    | 16     |
| Zr                             | 117    | 112   | 115    |
| Nb                             | 10.7   | 10.6  | 11.3   |
| <b>CIPW Norms.</b>             |        |       |        |
| Ap                             | 0.45   | 0.45  | 0.42   |
| Il                             | 3.55   | 3.45  | 3.52   |
| Mt                             | 9.32   | 9.29  | 9.31   |
| Or                             | 3.03   | 2.96  | 3.41   |
| Ab                             | 20.2   | 19.96 | 20.26  |
| An                             | 25.97  | 26.03 | 26.28  |
| Di                             | 20.67  | 20.32 | 20.76  |
| Hy                             | 9.73   | 8.97  | 9.5    |
| Cl                             |        |       |        |
| Ac                             |        |       |        |
| C                              |        |       |        |
| Q                              | 6.86   | 7.58  | 6.4    |



"HOUGHTON" GRANULITE

| SAMPLE #                       | O66   | 101   | 127   | B95   | HT    |
|--------------------------------|-------|-------|-------|-------|-------|
| Major element (Wt%).           |       |       |       |       |       |
| SiO <sub>2</sub>               | 61.99 | 59.74 | 58.92 | 57.89 | 58.84 |
| Al <sub>2</sub> O <sub>3</sub> | 15.7  | 12.83 | 13.99 | 15.04 | 15.69 |
| Fe <sub>2</sub> O <sub>3</sub> | 2.8   | 11.25 | 11.51 | 12.53 | 11.15 |
| MnO                            | 0.03  | 0.05  | 0.03  | 0     | 0.01  |
| MgO                            | 3.95  | 3.98  | 2.53  | 2.6   | 1.17  |
| CaO                            | 5.65  | 2.67  | 2.2   | 1.65  | 1.2   |
| Na <sub>2</sub> O              | 7.34  | 5.73  | 4.78  | 7.73  | 5.76  |
| K <sub>2</sub> O               | 1.7   | 2.41  | 4.51  | 1.13  | 4.83  |
| TiO <sub>2</sub>               | 0.24  | 0.6   | 0.64  | 0.57  | 0.65  |
| P <sub>2</sub> O <sub>5</sub>  | 0.15  | 0.15  | 0.16  | 0.15  | 0.19  |
| H <sub>2</sub> O-              | 0.38  | 0.52  | 0.52  | 0.47  | 0.34  |
| TOTAL                          | 99.94 | 99.93 | 99.79 | 99.78 | 99.84 |
| Trace elements (ppm).          |       |       |       |       |       |
| Sr                             | 157   | 12.9  | 34    | 17.6  | 55    |
| Rb                             | 39    | 52    | 98    | 23    | 83    |
| Y                              | 85    | 45    | 51    | 29    | 54    |
| Ba                             | 306   | 97    | 319   | 37    | 289   |
| Sc                             | 22    | 21    | 15.8  | 16.7  | 15    |
| Ni                             | 15    | 32    | 18    | 36    | 16    |
| V                              | 202   | 19    | 66    | 60    | 66    |
| Cr                             | 62    | 51    | 53    | 50    | 59    |
| Ga                             | 36    | 22    | 21    | 26    | 19    |
| Ce                             | 70    | 77    | 78    | 72    | 94    |
| Nd                             | 55    | 55    | 52    | 29    | 52    |
| La                             | 24    | 39    | 34    | 31    | 45    |
| Zr                             | 125   | 136   | 159   | 128   | 115   |
| Nb                             | 0.2   | 9.6   | 9     | 7.9   | 10.9  |
| CIPW Norms.                    |       |       |       |       |       |
| Ap                             | 0.32  | 0.36  | 0.37  | 0.34  | 0.44  |
| Il                             | 0.45  | 1.23  | 1.3   | 1.12  | 1.3   |
| Mt                             | 1.53  | 6.8   | 6.84  | 7.11  | 6.56  |
| Or                             | 9.8   | 15.39 | 28.37 | 6.91  | 30    |
| Ab                             | 60.59 | 24.41 | 43.07 | 67.72 | 51.25 |
| An                             | 4.75  | 13.26 | 3.62  | 3.11  | 2.83  |
| Di                             | 18.97 |       | 5.75  | 3.62  | 1.73  |
| Hy                             | 0.17  | 10.66 | 6.58  | 3.58  | 4.25  |
| Cl                             | 2.98  |       |       | 5.52  | 1.12  |
| Ac                             |       |       |       |       |       |
| C                              |       | 2.89  |       |       |       |
| Q                              |       | 21.36 | 3.37  |       |       |

APPENDIX 3  
ELECTRON MICROPROBE ANALYSIS AND  
MINERAL COMPOSITIONS

## PROCEDURE

Polished thin sections were coated with approximately 250um of carbon. Analyses of each grain were carried out using a KEVEX 7000 Series energy dispersive system attached to a JEOL<sup>1</sup>733 Analyser.

Analyses conditions used were 15kV accelerating voltage and 5nA electron beam current and data was corrected on-line using PIBS style software.

Calibration of the KEVEX EDS system was carried out using pure copper as a primary standard.

### Samples analysed.

|         |   |                       |
|---------|---|-----------------------|
| 896-26  | - | Sillimanite gneiss    |
| 896-32  | - | Sillimanite gneiss    |
| 896-50  | - | Amphibolite           |
| 896-11  | - | Aplite/Microgranite   |
| 896-066 | - | Pyroxene-Amphibole    |
| 896-66  | - | Quartz-biotite gneiss |

Average analysis of probed thin sections  
 Sample 896-26 Sillimanite Gneiss

|                                | Biotite | Biotite edge | Garnet | Garnet edge | K-feldspar |
|--------------------------------|---------|--------------|--------|-------------|------------|
| SiO <sub>2</sub>               | 36.7    | 35.71        | 36.45  | 36          | 44.76      |
| TiO <sub>2</sub>               | 1.49    | 1.52         | -      | -           | 0.3        |
| Al <sub>2</sub> O <sub>3</sub> | 17.01   | 17.41        | 20.32  | 20.28       | 33.66      |
| FeO                            | 16.29   | 14.93        | 28.28  | 27.93       | 2.77       |
| MnO                            | -       | -            | 9.21   | 9.75        | -          |
| MgO                            | 11.14   | 9.85         | 3.15   | 2.66        | 0.81       |
| K <sub>2</sub> O               | 9.07    | 8.06         | -      | -           | 10.21      |
| CaO                            | -       | -            | 0.76   | 0.79        | -          |
| Na <sub>2</sub> O              | 0.16    | 0.37         | 0.43   | 0.34        | 1.07       |
| TOTAL                          | 92.52   | 88.65        | 98.6   | 97.91       | 93.57      |

Structural Formulae

| oxygen per<br>formula unit | 22      | 22      | 12     | 12     | 8      |
|----------------------------|---------|---------|--------|--------|--------|
| Si                         | 5.6923  | 5.7623  | 2.992  | 2.979  | 2.2305 |
| Ti                         | 0.1734  | 0.2013  | -      | -      | 0.0112 |
| Al                         | 3.1065  | 3.6491  | 1.9653 | 1.9775 | 1.9767 |
| Fe                         | 2.1124  | 2.1771  | 1.9413 | 1.9325 | 0.1153 |
| Mn                         | -       | -       | 0.6404 | 0.6833 | -      |
| Mg                         | 2.5747  | 2.4911  | 0.386  | 0.3281 | 0.06   |
| K                          | 1.7934  | 1.806   | -      | -      | 0.6488 |
| Ca                         | -       | -       | 0.0655 | 0.696  | -      |
| Na                         | 0.0495  | 0.1482  | 0.0677 | 0.0542 | 0.1035 |
| TOTAL                      | 16.6806 | 16.2351 | 8.0591 | 8.0347 | 5.146  |

Sample 896-32 Sillimanite gneiss

|                                | Biotope | K-feldspar | plagioclase |
|--------------------------------|---------|------------|-------------|
| SiO <sub>2</sub>               | 35.61   | 45.49      | 63.25       |
| TiO <sub>2</sub>               | 1.69    | 0.19       | -           |
| Al <sub>2</sub> O <sub>3</sub> | 17.06   | 34.24      | 24.57       |
| FeO                            | 17.55   | 2.61       | -           |
| MnO                            | -       | -          | -           |
| MgO                            | 11.32   | 0.8        | -           |
| K <sub>2</sub> O               | 9.46    | 10.43      | 0.16        |
| CaO                            | -       | -          | 5.43        |
| Na <sub>2</sub> O              | 0.26    | 0.9        | 8.56        |
| TOTAL                          | 94.17   | 94.71      | 102.37      |

Structural formulae

oxygen per  
formula unit

|       | 22     | 8      | 8      |
|-------|--------|--------|--------|
| Si    | 5.5268 | 2.2368 | 2.7531 |
| Ti    | 0.1974 | 0.0069 | -      |
| Al    | 3.1207 | 1.9843 | 1.2523 |
| Fe    | 2.2774 | 0.1071 | -      |
| Mn    | -      | -      | -      |
| Mg    | 2.6175 | 0.0587 | -      |
| K     | 1.8722 | 0.6544 | 0.0087 |
| Ca    | -      | -      | 0.2519 |
| Na    | 0.3236 | 0.0859 | 0.7182 |
| TOTAL | 16.014 | 5.1392 | 5.056  |

Sample 896-50 Amphibolite

|                                | Ilmenite | plagioclase | Amphibole |
|--------------------------------|----------|-------------|-----------|
| SiO <sub>2</sub>               | 0.28     | 60.57       | 52.76     |
| TiO <sub>2</sub>               | 48.37    | -           | -         |
| Al <sub>2</sub> O <sub>3</sub> | 0.12     | 25.64       | 3.75      |
| FeO                            | 46.69    | -           | 16.86     |
| V <sub>2</sub> O <sub>3</sub>  | 0.38     | -           | -         |
| MgO                            | 0.31     | -           | 12.59     |
| K <sub>2</sub> O               | -        | 0.1         | 0.16      |
| CaO                            | -        | 6.92        | 11.95     |
| Na <sub>2</sub> O              | 0.36     | 7.72        | 0.7       |
| MnO                            | 1.64     | -           | 0.33      |
| TOTAL                          | 98.29    | 100.95      | 99.1      |

Structural Formulae

| oxygen per<br>formula unit | 3      | 8      | 6      |
|----------------------------|--------|--------|--------|
| Si                         | 0.073  | 2.6708 | 1.9925 |
| Ti                         | 0.9947 | 1.3326 | -      |
| Al                         | 0.0036 | 0.3267 | 0.1668 |
| Fe                         | 1.014  | -      | 0.5323 |
| Mn                         | 0.036  | -      | 0.0105 |
| Mg                         | 0.0119 | -      | 0.7086 |
| K                          | -      | 0.0058 | 0.0079 |
| Ca                         | -      | 0.3267 | 0.4836 |
| Na                         | 0.0181 | 0.6597 | 0.0514 |
| V                          | 0.0079 | -      | -      |
| TOTAL                      | 2.0466 | 4.9956 | 3.9537 |

sample 896-11 Aplite/Microgranite

|                                | K-feldspar | plagioclase | Biotite |
|--------------------------------|------------|-------------|---------|
| SiO <sub>2</sub>               | 64.3       | 68.78       | 35.71   |
| TiO <sub>2</sub>               | -          | -           | 2.48    |
| Al <sub>2</sub> O <sub>3</sub> | 17.79      | 20.47       | 15.52   |
| FeO                            | -          | -           | 20.48   |
| MgO                            | -          | -           | 9.94    |
| K <sub>2</sub> O               | 15.06      | 0.42        | 9.63    |
| CaO                            | -          | 0.95        | -       |
| Na <sub>2</sub> O              | 0.79       | 10.86       | -       |
| TOTAL                          | 98.11      | 101.49      | 95.56   |

Structural Formulae

| oxygen per<br>formula unit | 8      | 8      | 22      |
|----------------------------|--------|--------|---------|
| Si                         | 3.0128 | 2.9651 | 5.5849  |
| Ti                         | -      | -      | 0.292   |
| Al                         | 0.9924 | 1.0401 | 2.8601  |
| Fe                         | -      | -      | 2.6792  |
| Mg                         | -      | -      | 2.3161  |
| K                          | 0.9    | 0.0232 | 1.921   |
| Ca                         | -      | -      | -       |
| Na                         | 0.0715 | 0.9081 | -       |
| TOTAL                      | 4.9767 | 4.9805 | 16.1306 |

sample 896-066 Pyroxene-amphibole granulite

Plagioclase      amphibole      Haematite

|                                |        |        |       |
|--------------------------------|--------|--------|-------|
| SiO <sub>2</sub>               | 68.68  | 56.26  | 0.12  |
| Al <sub>2</sub> O <sub>3</sub> | 21.18  | 0.3    | 88.87 |
| FeO                            | -      | 6.31   | 0.19  |
| MgO                            | -      | 14.54  | -     |
| K <sub>2</sub> O               | 0.25   | -      | -     |
| CaO                            | 1.61   | 23.92  | -     |
| Na <sub>2</sub> O              | 10.73  | 0.64   | -     |
| TOTAL                          | 102.44 | 101.96 | 91.53 |

structural Formulae

oxygen per  
formula unit

8

6

3

|       |        |        |        |
|-------|--------|--------|--------|
| Si    | 2.9368 | 2.0306 | 0.0054 |
| Al    | 0.0138 | 0.0126 | 0.0096 |
| Fe    | -      | 0.1904 | 2.866  |
| Mg    | -      | 0.7821 | 0.0111 |
| K     | 0.0138 | -      | -      |
| Ca    | 0.0739 | 0.9252 | -      |
| Na    | 0.8893 | 0.0445 | 0.0286 |
| TOTAL | 4.9811 | 3.9853 | 2.9766 |



Sample 896-66 Quartz-biotite gneiss

Biotite                      Altered K-spar

|                                |       |       |
|--------------------------------|-------|-------|
| SiO <sub>2</sub>               | 36.12 | 42.6  |
| TiO <sub>2</sub>               | 2.23  | 0.71  |
| Al <sub>2</sub> O <sub>3</sub> | 17.35 | 30.46 |
| FeO                            | 15.8  | 5.48  |
| MgO                            | 11.9  | 2.68  |
| K <sub>2</sub> O               | 9.73  | 10.24 |
| CaO                            | -     | -     |
| Na <sub>2</sub> O              | 0.46  | 0.64  |
| TOTAL                          | 93.99 | 93.02 |

Structural formulae

oxygen per  
formula unit

24

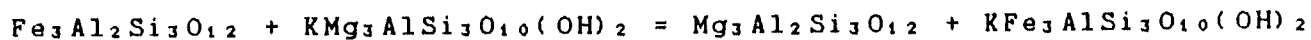
8

|       |         |        |
|-------|---------|--------|
| Si    | 6.0249  | 2.1877 |
| Ti    | 0.2798  | 0.0273 |
| Al    | 3.4114  | 1.8433 |
| Fe    | 2.2038  | 0.2354 |
| Mg    | 2.9603  | 0.2021 |
| K     | 2.0701  | 0.6707 |
| Ca    | -       | -      |
| Na    | 0.1474  | 0.0641 |
| TOTAL | 17.2134 | 5.2526 |

APPENDIX 4  
GEOTHERMOMETRY  
AND  
GEOBAROMETRY

A) Ferry and Spear (1978)

They investigated the partitioning of Fe and Mg between synthetic garnet and synthetic biotite, considering the cation exchange reaction :



Almandine                      Mg-biotite                      Pyrope                      Fe-biotite

Numerical analysis of the experimental data yielded a geothermometer for the rocks containing biotite and garnet, that are close to binary Fe-Mg compounds.

$$12,454 - 4.662T(\text{K}) + 0.057P(\text{bars}) + 3RT\ln K_0 = 0$$

As  $K_0$  is also a function of the Ca and Mn content in garnet, and the Ti and Al(VI) content in biotite, they suggest the following limitations on the geothermometer. It can be used

$$\text{if } \frac{(\text{Ca} + \text{Mn})}{(\text{Ca} + \text{Mn} + \text{Fe} + \text{Mg}) \text{ garnet}} < 0.2 \quad \text{ie } x^{\text{garnet}}_{\text{Ca} + \text{Mn}} < 0.2$$

$$\text{and } \frac{(\text{Ti} + \text{Al(VI)})}{(\text{Ti} + \text{Al(VI)} + \text{Fe} + \text{Mg}) \text{ biotite}} < 0.15 \quad \text{ie } x^{\text{biotite}}_{\text{Ti} + \text{Al(VI)}} < 0.15$$

His geothermometer is applicable below 800°C and has an error range of  $\pm 50^\circ\text{C}$ .

Ganguly and Saxena (1984)

They gave the following equations and modifications to Ferry and Spear's (1978) Gt-Bt equilibrium.

Equation (1) can be combined with the thermodynamic expression of  $\ln K$  as a function of P and T to yield the following relation between T and  $K_0$  involving garnet and a co-existing phase  $\alpha$  for a compositional range over which garnet can be approximated by a symmetrical solution model, i. e. equation (2).

$$RT\ln K_0 = RT\ln K_0(P, T) + [W_{\text{Fe-Mg}}(X_{\text{Fe}} - X_{\text{Mg}}) + \sum(W_{\text{Mg-K}} - W_{\text{Fe-K}})(X_{\text{K}})]^{\text{Gt}} \quad (1) \\ + [W_{\text{Fe-Mg}}(X_{\text{Mg}\alpha} - X_{\text{Fe}\alpha}) + \sum(W_{\text{Fe}\alpha} - W_{\text{Mg}\alpha})(X_{\text{L}})]^{\alpha}$$

(where  $K_0$  is the  $\text{Fe}^{2+}$ - $\text{Mg}^{2+}$  distribution coefficient between two

co-existing phases)

$$T(K) = A + \frac{[W_{Fe,Mg} (X_{Fe} - X_{Mg}) + \Delta W_{Ca} X_{Ca} + \Delta W_{Mn} X_{Mn}]^{6t}}{\ln K_0 - \Delta S^0/R - \ln(Y_{Fe}/Y_{Mg})^{6t}} / R \quad (2)$$

(where A stands for 1/T in the thermodynamic expression of lnK)

Thus, combining F and S, the expression for lnK<sub>0</sub> vs 1/T with equation (1), we obtain;

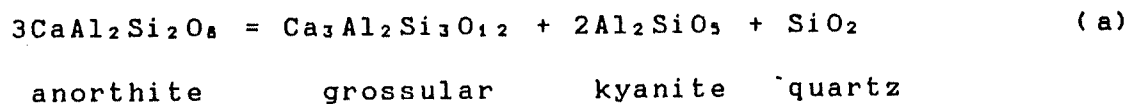
$$\ln K(P, T) = 2089 - 0.8 \frac{W_{Fe,Mg}}{T} / R + 9.45P(Kb) - 0.782 \quad (3)$$

The expression of A (coefficient of 1/T) and \*S<sup>0</sup>/R (= -0.782) in equation (3) may now be substituted in equation (2), giving;

$$W_{Fe,Mg}^{6t} = W_{Fe,Mg}^{F-Mg} [Mg/(Mg + Fe^{2+})]^{6t} + W_{Mg-Fe} [Fe^{2+}/(Fe^{2+} + Mg)]^{6t}$$

Newton and Hasselton (1981) - a variation of Saxena and Ribbie

The garnet - kyanite - plagioclase barometer is based on the equilibrium equation;



They derived the following expression for this equilibrium state;

$$P = \frac{[P^0 \Delta V^0 - 3RT \ln a_{Ca}^{6t} / a_{An}^{12t}]}{\Delta V(a)}$$

where activities are at 1 bar, T, and P<sup>0</sup> is the equilibrium pressure of (a) when all components are in their respective pure states.

Indares and Martignole (1985)

Their corrections are made for Ti and Al substitutions in biotite. Ti and Al interaction parameters have been evaluated as;

$$m = (W_{FeAl}^{Bi} - W_{MgAl}^{Bi}) = -464 \text{ or } -1590 \text{ and } n = (W_{FeTi}^{Bi} - W_{MgTi}^{Bi}) = -6767 \text{ or } -7451$$

(in cal. per mole) depending on the model adopted for the non-ideality in garnet. Starting from the experimental ideal model of Ferry and Spear (1978), a new calibration of the biotite - garnet geothermometer based upon the above correction for Al and Ti and

the interaction of Ca in Fe-Mg garnets is proposed here;

$$T^{\circ}K = 12454 + 0.057P(\text{bars}) + 3(mX_{\text{Al}}^{b_i} + nX_{\text{Ti}}^{b_i}) - (\Delta W_{\text{Ca}} X_{\text{Ca}}^{a_i} + \Delta W_{\text{Mn}} + X_{\text{Ca}}^{a_i}) \\ 4.662 - 5.9616 \ln K_0$$

Starting from the experimentally derived equation of Ferry and Spear (1978), two more elaborated expressions of the  $\ln K_0$  vs  $1/T$  relationships, depending on the correction model for garnet, can now be formulated for deviations from ideality in both garnet and biotite solid solution.

Model A:  $T^{\circ}K = 12454 + 0.057P(\text{bar}) + 3(-454X_{\text{Al}}^{b_i} - 6767X_{\text{Ti}}^{b_i}) - 3(-3000 - 1.5T) X_{\text{Ca}}^{a_i}$

Model B:  $T^{\circ}K = 12454 + 0.057P(\text{bar}) + 3(-1590X_{\text{Al}}^{b_i} - 7451X_{\text{Ti}}^{b_i}) - 3(-3000(X_{\text{Ca}}^{a_i} + X_{\text{Mn}}^{a_i}))$

Results were obtained by use of computer programs developed by R. Lawrence and Powell and Holland.

Garnet Plagioclase Sillimanite Quartz Geobarometer  
 GROSSULAR ACTIVITY calculated using the method of  
 Newton and Haselton (1981)  
 ANORTHITE ACTIVITY calculated using the methods of:  
 Newton and Haselton (1981) and  
 Saxena and Ribbie (1972)

Sample Name:

Components of Garnet:  
 Gross Pyrope Alman Spess  
 2.70454E-02 .140579 .594893 .237483

An in Plagioclase: 4.11515E-02

Partial molar volume of reaction: 70.4231 cm cubed

| T°C  | Activity Gross | PRESSURE ESTIMATES (kbar) using plagioclase |         |
|------|----------------|---|---------|
|      |                | N&H '81                                     | S&R '72 |
| 500  | 4.09634E-02    | 8.71094                                     | 6.56479 |
| 600  | 3.99347E-02    | 11.3254                                     | 8.71678 |
| 700  | 3.91358E-02    | 13.9398                                     | 10.8688 |
| 800  | 3.84976E-02    | 16.5542                                     | 13.0208 |
| 900  | 3.79762E-02    | 19.1687                                     | 15.1727 |
| 1000 | 3.75421E-02    | 21.7831                                     | 17.3247 |

Table 4

Garnet Biotite Geothermometry using various parameters

Sample Name: 896-26

Gross. 2.38612E-02  
 Garnet Composition  
 Pyrope .144613      Alman. .614606  
 Spess. .21692

X-Ti: .038835  
 Biotite Composition  
 X-Al: .127832      X-Fe: .372168  
 X-Mg: .461165

Corrections of Indares and Martignole (1985)  
 Model A. For biotite: -66.3409      For garnet: 16.3379  
 Model B. For biotite: -101.457      For garnet: 148.772  
 Correction for non-ideal Fe and Mg mixing  
 according to the model of Ganguly and Saxena (1984): -181.295

| P (kb) | T (F&S'78) | (Model A) | (Model B) | Non-ideal Fe&I |
|--------|------------|-----------|-----------|----------------|
| 4      | 597.5      | 547.497   | 644.815   | 564.977 °C     |
| 6      | 605.327    | 555.324   | 652.641   | 572.804 °C     |
| 8      | 613.153    | 563.15    | 660.468   | 580.63 °C      |
| 10     | 620.979    | 570.976   | 668.294   | 588.457 °C     |
| 12     | 628.806    | 578.803   | 676.12    | 596.283 °C     |

Gross. 2.40935E-02  
 Garnet Composition  
 Pyrope .139749      Alman. .63162  
 Spess. .204537

X-Ti: .032417  
 Biotite Composition  
 X-Al: .166828      X-Fe: .367969  
 X-Mg: .432786

Corrections of Indares and Martignole (1985)  
 Model A. For biotite: -60.8896      For garnet: 16.4348  
 Model B. For biotite: -103.98      For garnet: 140.726  
 Correction for non-ideal Fe and Mg mixing  
 according to the model of Ganguly and Saxena (1984): -169.188

| P (kb) | T (F&S'78) | (Model A) | (Model B) | Non-ideal Fe&I |
|--------|------------|-----------|-----------|----------------|
| 4      | 594.179    | 549.724   | 630.925   | 565.717 °C     |
| 6      | 601.976    | 557.521   | 638.721   | 573.514 °C     |
| 8      | 609.772    | 565.317   | 646.518   | 581.31 °C      |
| 10     | 617.569    | 573.114   | 654.314   | 589.107 °C     |
| 12     | 625.365    | 580.91    | 662.111   | 596.903 °C     |

Gross. 2.36991E-02  
 Garnet Composition  
 Pyrope .138327      Alman. .622643  
 Spess. .215331

X-Ti: .032417  
 Biotite Composition  
 X-Al: .166828      X-Fe: .367969  
 X-Mg: .432786

Corrections of Indares and Martignole (1985)  
 Model A. For biotite: -60.9911      For garnet: 16.1909  
 Model B. For biotite: -104.153      For garnet: 147.372  
 Correction for non-ideal Fe and Mg mixing  
 according to the model of Ganguly and Saxena (1984): -172.843

| P (kb) | T (F&S'78) | (Model A) | (Model B) | Non-ideal Fe&I |
|--------|------------|-----------|-----------|----------------|
| 4      | 595.625    | 550.825   | 638.843   | 570.154 °C     |
| 6      | 603.434    | 558.634   | 646.653   | 577.963 °C     |
| 8      | 611.244    | 566.444   | 654.462   | 585.773 °C     |
| 10     | 619.053    | 574.253   | 662.272   | 593.582 °C     |
| 12     | 626.863    | 582.063   | 670.081   | 601.392 °C     |

Garnet Composition  
 Gross. Pyrope Alman. Spess.  
 2.22803E-02 .141371 .61884 .21751

Biotite Composition  
 X-Ti: X-Al: X-Fe: X-Mg:  
 .032417 .166828 .367969 .432786

Corrections of Indares and Martignole (1985)  
 Model A. For biotite: -61.6939 For garnet: 15.3914  
 Model B. For biotite: -105.354 For garnet: 149.544  
 Correction for non-ideal Fe and Mg mixing  
 according to the model of Ganguly and Saxena (1984): -178.754

| P (kb) | T (F&S'78) | (Model A) | (Model B) | Non-ideal Fe&Mg |
|--------|------------|-----------|-----------|-----------------|
| 4      | 605.636    | 559.334   | 649.826   | 576.426 °C      |
| 6      | 613.536    | 567.233   | 657.726   | 584.326 °C      |
| 8      | 621.435    | 575.133   | 665.626   | 592.225 °C      |
| 10     | 629.335    | 583.032   | 673.525   | 600.125 °C      |
| 12     | 637.234    | 590.932   | 681.424   | 608.024 °C      |

Garnet Composition  
 Gross. Pyrope Alman. Spess.  
 2.40935E-02 .139749 .63162 .204537

Biotite Composition  
 X-Ti: X-Al: X-Fe: X-Mg:  
 3.41269E-02 .159314 .351976 .454583

Corrections of Indares and Martignole (1985)  
 Model A. For biotite: -60.2497 For garnet: 15.8265  
 Model B. For biotite: -100.316 For garnet: 135.554  
 Correction for non-ideal Fe and Mg mixing  
 according to the model of Ganguly and Saxena (1984): -162.97

| P (kb) | T (F&S'78) | (Model A) | (Model B) | Non-ideal Fe&Mg |
|--------|------------|-----------|-----------|-----------------|
| 4      | 562.306    | 517.883   | 597.544   | 534.89 °C       |
| 6      | 569.816    | 525.393   | 605.054   | 542.4 °C        |
| 8      | 577.326    | 532.903   | 612.564   | 549.91 °C       |
| 10     | 584.836    | 540.413   | 620.074   | 557.42 °C       |
| 12     | 592.346    | 547.923   | 627.584   | 564.93 °C       |

Garnet Composition  
 Gross. Pyrope Alman. Spess.  
 2.77948E-02 .123568 .587496 .261142

Biotite Composition  
 X-Ti: X-Al: X-Fe: X-Mg:  
 3.70488E-02 .130048 .367043 .465861

Corrections of Indares and Martignole (1985)  
 Model A. For biotite: -60.6817 For garnet: 18.0406  
 Model B. For biotite: -94.1926 For garnet: 169.102  
 Correction for non-ideal Fe and Mg mixing  
 according to the model of Ganguly and Saxena (1984): -170.689

| P (kb) | T (F&S'78) | (Model A) | (Model B) | Non-ideal Fe&Mg |
|--------|------------|-----------|-----------|-----------------|
| 4      | 551.544    | 508.903   | 626.453   | 549.957 °C      |
| 6      | 558.957    | 516.316   | 633.867   | 557.37 °C       |
| 8      | 566.37     | 523.729   | 641.28    | 564.783 °C      |
| 10     | 573.783    | 531.142   | 648.693   | 572.197 °C      |
| 12     | 581.197    | 538.556   | 656.107   | 579.61 °C       |

APPENDIX 5  
GEOCHRONOLOGICAL TECHNIQUES  
AND DETAILED RESULTS



## ISOTOPE EXTRACTION

Six of the above magnetic and size fractions were chosen as to give as wide a range in size and magnetic susceptibility as possible.

Each fraction was purified by handpicking.

From three to nine milligrams of each fraction was dissolved under pressure in a mixture of HF and HNO<sub>3</sub> at 220 C for one week.

Each of the six solutions was then divided into two fractions and a mixed U/Pb spike was added to one of these.

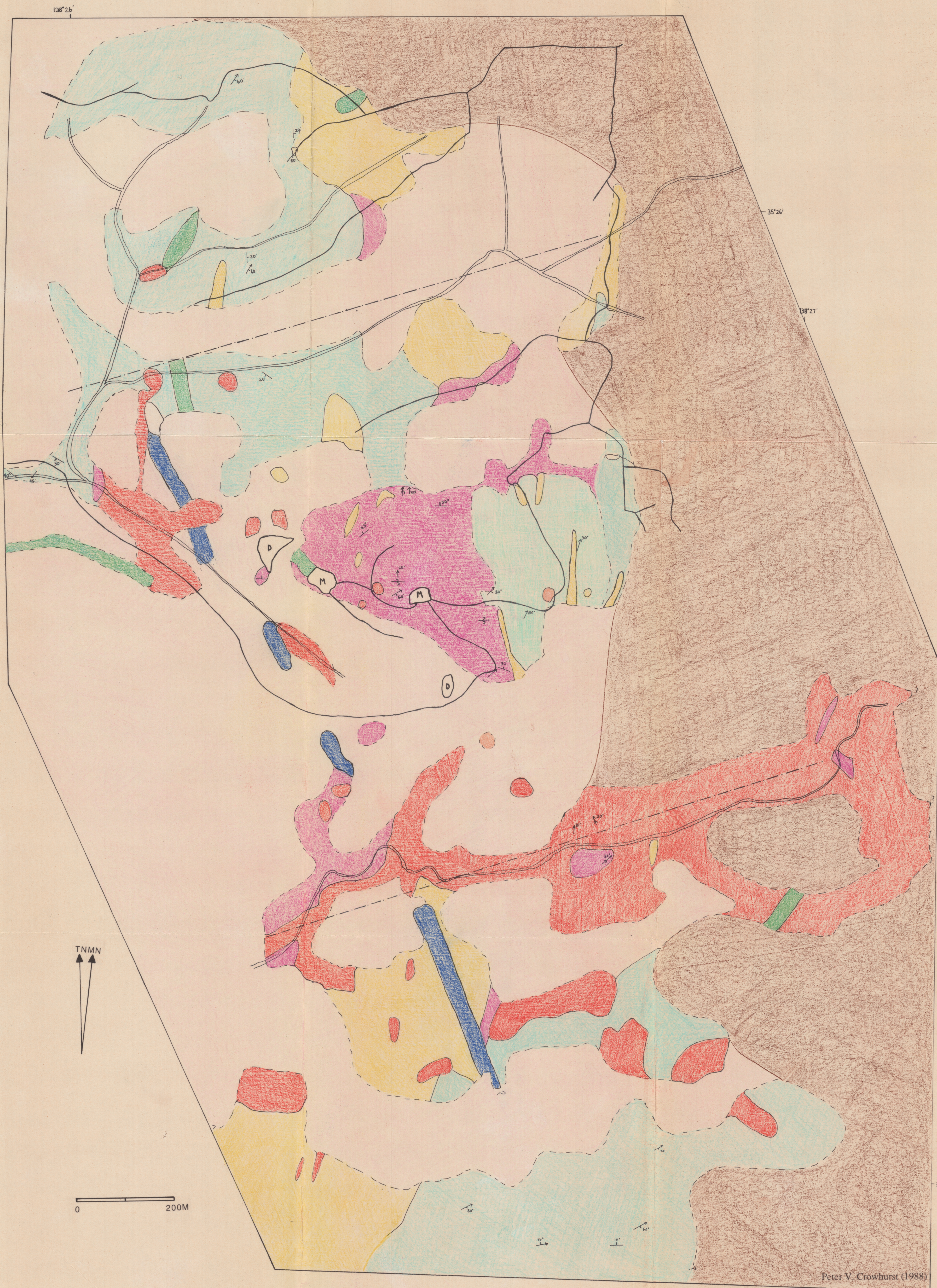
The spiked and unspiked were run through ion exchange columns and the Pb, Pb-spiked and U-spiked fractions collected.

Pb and Pb-spiked fractions were loaded onto rhenium filament beads and U-spiked fractions were loaded onto tantalum filament beads and analysed on the mass spectrometer.

| Zircon fraction | Size (microns) | Magnetic response | Weight (mg) | U (ppm) | Pb (ppm) | Apparent ages (Ma)                  |                                     |                                    |                                    |                                     |                                    |                                    |                                     |  |  |
|-----------------|----------------|-------------------|-------------|---------|----------|-------------------------------------|-------------------------------------|------------------------------------|------------------------------------|-------------------------------------|------------------------------------|------------------------------------|-------------------------------------|--|--|
|                 |                |                   |             |         |          | $\frac{206\text{Pb}}{204\text{Pb}}$ | $\frac{206\text{Pb}}{208\text{Pb}}$ | $\frac{206\text{Pb}}{238\text{U}}$ | $\frac{207\text{Pb}}{235\text{U}}$ | $\frac{207\text{Pb}}{206\text{Pb}}$ | $\frac{206\text{Pb}}{238\text{U}}$ | $\frac{207\text{Pb}}{235\text{U}}$ | $\frac{207\text{Pb}}{206\text{Pb}}$ |  |  |
| 1               | >250           | a11               | 15.2        | 1326    | 260      | 6171                                | 12.91                               | 0.1929                             | 2.577                              | 0.09692                             | 1137                               | 1294                               | 1566                                |  |  |
| 2               | 142 - 250      | NM 0              | 9.3         | 788     | 179      | 2087                                | 12.95                               | 0.2188                             | 2.916                              | 0.09665                             | 1275                               | 1386                               | 1560                                |  |  |
| 3               | 142 - 250      | M 0               | 11.9        | 1415    | 255      | 4893                                | 18.54                               | 0.1798                             | 2.388                              | 0.09621                             | 1066                               | 1239                               | 1554                                |  |  |
| 4               | 105 - 142      | M 0               | 5.7         | 1644    | 263      | 2386                                | 18.22                               | 0.1578                             | 2.078                              | 0.09552                             | 945                                | 1142                               | 1538                                |  |  |
| 5               | 105 - 142      | NM 0              | 11.5        | 1007    | 212      | 4849                                | 15.27                               | 0.2085                             | 2.774                              | 0.09647                             | 1221                               | 1349                               | 1557                                |  |  |
| 7               | 75 - 105       | NM 0              | 22.3        | 818     | 179      | 8081                                | 12.80                               | 0.2147                             | 2.876                              | 0.09714                             | 1254                               | 1376                               | 1570                                |  |  |

TABLE 5 : U - Pb isotopic analyses of zircon fractions separated from the Leura Hills aplite 896 - 11 Under "Magnetic response" M = magnetic, NM = non-magnetic, and the digit represents degrees dip of the Franz separator magnet with 1.8 amps magnet current. The  $206\text{Pb}/204\text{Pb}$  ratio is as measured. The other isotope ratios include radiogenic lead only.

FIG. 18 GEOLOGY OF PART OF THE YANKALILLA-MYPONGA INLIER, S.A.



LEGEND

PROTEROZOIC INLIER

- |               |  |   |
|---------------|--|---|
| Metasediments |  | Quartz - Biotite Gneiss                                     |
|               |  | Sillimanite Gneiss  |
|               |  | Quartzo-feldspathic Gneiss/<br>Amphibole-pyroxene Granulite |
|               |  | Quartz-Biotite Schist                                       |
| Intrusives    |  | Amphibolite   |
|               |  | Pegmatite   |
|               |  | Aplite/Microgranite   |

PERMIAN

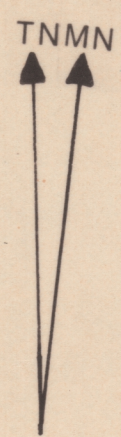
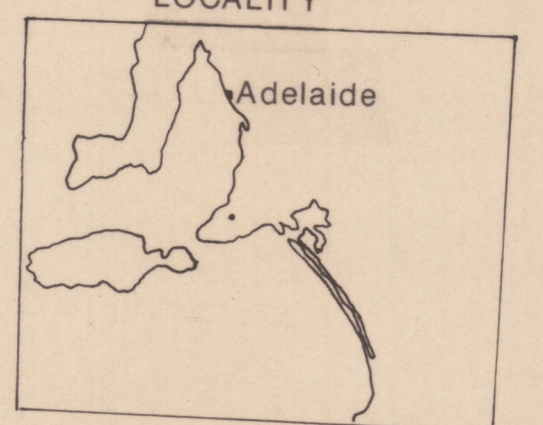
- |  |                   |
|--|-------------------|
|  | Sandstone/Tillite |
|--|-------------------|

QUATERNARY

- |  |                     |
|--|---------------------|
|  | Lateritic sandstone |
|--|---------------------|

- |   |                               |
|---|-------------------------------|
|   | Geological Boundary           |
|   | Inferred Boundary             |
|   | Strike and Dip of Strata      |
|   | Strike and Dip of Schistosity |
|   | Creek                         |
|   | Vehicle Track                 |
|   | plunge of fold                |
|   | isoclinal folding             |
|   | inferred faults               |
| M | Mine                          |
| D | Dam                           |

LOCALITY



0 200M